

MOISTURE TRANSPORT REVIEW

Cementitious Barriers Partnership

November 2009

CBP-TR-2009-002-C6, Rev. 0

ACKNOWLEDGEMENTS

This report was prepared for the United States Department of Energy in part under Contract No. DE-AC09-08SR22470 and is an account of work performed in part under that contract. This report was prepared in support of the Savannah River Nuclear Solutions Cooperative Research Agreement (CRADA) CR-08-001. Reference herein to any specific commercial product, process, or service by trademark, name, manufacturer, or otherwise does not necessarily constitute or imply endorsement, recommendation, or favoring of same by Savannah River Nuclear Solutions or by the United States Government or any agency thereof. The views and opinions of the authors expressed herein do not necessarily state or reflect those of the United States Government or any agency thereof.

and

This report is based in part on work supported by the United States Department of Energy under Cooperative Agreement Number DE-FC01-06EW07053 entitled “The Consortium for Risk Evaluation with Stakeholder Participation III” awarded to Vanderbilt University. The opinions, findings, conclusions, or recommendations expressed herein are those of the author(s) and do not necessarily represent the views of the Department of Energy or Vanderbilt University.

Disclaimer

This work was prepared under an agreement with and funded by the U. S. Government. Neither the U.S. Government or its employees, nor any of its contractors, subcontractors or their employees, makes any express or implied: 1. warranty or assumes any legal liability for the accuracy, completeness, or for the use or results of such use of any information, product, or process disclosed; or 2. representation that such use or results of such use would not infringe privately owned rights; or 3. endorsement or recommendation of any specifically identified commercial product, process, or service. Any views and opinions of authors expressed in this work do not necessarily state or reflect those of the United States Government, or its contractors, or subcontractors, or subcontractors.

Printed in the United States of America

**United State Department of Energy
Office of Environmental Management
Washington, DC**

This document is available on the CBP website: <http://cementbarriers.org/>

and

Savannah River National Laboratory website: <http://srnl.doe.gov>

FOREWORD

The Cementitious Barriers Partnership (CBP) Project is a multi-disciplinary, multi-institutional collaboration supported by the United States Department of Energy (US DOE) Office of Waste Processing. The objective of the CBP project is to develop a set of tools to improve understanding and prediction of the long-term structural, hydraulic, and chemical performance of cementitious barriers used in nuclear applications.

A multi-disciplinary partnership of federal, academic, private sector, and international expertise has been formed to accomplish the project objective. In addition to the US DOE, the CBP partners are the United States Nuclear Regulatory Commission (NRC), the National Institute of Standards and Technology (NIST), the Savannah River National Laboratory (SRNL), Vanderbilt University (VU) / Consortium for Risk Evaluation with Stakeholder Participation (CRESP), Energy Research Center of the Netherlands (ECN), and SIMCO Technologies, Inc.

The periods of cementitious performance being evaluated are >100 years for operating facilities and > 1000 years for waste management. The set of simulation tools and data developed under this project will be used to evaluate and predict the behavior of cementitious barriers used in near-surface engineered waste disposal systems, e.g., waste forms, containment structures, entombments, and environmental remediation, including decontamination and decommissioning (D&D)

activities. The simulation tools also will support analysis of structural concrete components of nuclear facilities (spent-fuel pools, dry spent-fuel storage units, and recycling facilities such as fuel fabrication, separations processes). Simulation parameters will be obtained from prior literature and will be experimentally measured under this project, as necessary, to demonstrate application of the simulation tools for three prototype applications (waste form in concrete vault, high-level waste tank grouting, and spent-fuel pool). Test methods and data needs to support use of the simulation tools for future applications will be defined.

The CBP project is a five-year effort focused on reducing the uncertainties of current methodologies for assessing cementitious barrier performance and increasing the consistency and transparency of the assessment process. The results of this project will enable improved risk-informed, performance-based decision-making and support several of the strategic initiatives in the DOE Office of Environmental Management Engineering & Technology Roadmap. Those strategic initiatives include 1) enhanced tank closure processes; 2) enhanced stabilization technologies; 3) advanced predictive capabilities; 4) enhanced remediation methods; 5) adapted technologies for site-specific and complex-wide D&D applications; 6) improved SNF storage, stabilization and disposal preparation; 7) enhanced storage, monitoring and stabilization systems; and 8) enhanced long-term performance evaluation and monitoring.

Christine A. Langton, PhD.
Savannah River National Laboratory

David S. Kosson, PhD.
Vanderbilt University/CRESP

MOISTURE TRANSPORT REVIEW

J. R. Arnold

Email: j.arnold@vanderbilt.edu

and

A. C. Garrabrants

Email: a.garrabrants@vanderbilt.edu

Vanderbilt University, School of Engineering

Consortium for Risk Evaluation with Stakeholder Participation, III

Nashville, TN 37235

E. Samson

Email: esamson@simcotechologies.com

SIMCO Technology, Inc.

Quebec City, Canada

G. P. Flach

Email: gregory.flach@srnl.doe.gov

and

C. A. Langton

Email: christine.langton@srnl.doe.gov

Savannah River National Laboratory

Aiken, SC 29808

November 2009

CBP-TR-2009-002, Rev. 0

CONTENTS	Page No.
LIST OF FIGURES	VI-ix
LIST OF TABLES	VI-ix
LIST OF ABBREVIATIONS AND ACRONYMS	VI-x
LIST OF NOMENCLATURE	VI-xi
ABSTRACT	VI-1
1.0 INTRODUCTION	VI-1
2.0 BACKGROUND	VI-2
2.1 Morphology and Terminology	VI-2
2.2 Mechanisms of Moisture Transport	VI-3
2.2.1 Flow-Inducing Potentials.....	VI-3
2.2.2 Equilibrium Pressure Conditions.....	VI-4
2.3 Modeling Formulations	VI-4
3.0 MOISTURE TRANSPORT IN POROUS MEDIA	VI-5
3.1 Transport Equations	VI-5
3.2 Model Parameters	VI-6
3.2.1 Relative Permeability as a Function of Saturation	VI-6
3.2.2 Hydraulic Diffusivity as a Function of Water Content.....	VI-7
3.2.3 Hydraulic Diffusivity as a Function of Relative Humidity	VI-8
3.3 Selected Model Parameter Measurements	VI-11
3.3.1 Saturated Hydraulic Conductivity (Permeability)	VI-11
3.3.2 Porosity and Pore Size Distribution Measurements	VI-14
3.3.3 Measurement of Hydraulic Diffusivity.....	VI-15
3.4 Qualitative Tests	VI-16
4.0 MOISTURE TRANSPORT THROUGH FRACTURED MEDIA	VI-16
4.1 Role of Fractures in Moisture Transport	VI-17
4.1.1 Modeling Approaches for Fractured Media.....	VI-19
5.0 OTHER TRANSPORT MODELS	VI-21
5.1 Pore-scale Models	VI-21
5.2 Lattice-Boltzmann Methods	VI-22

CONTENTS (contd)	Page No.
6.0 CHALLENGES AND OPPORTUNITIES	VI-23
7.0 REFERENCES	VI-24
8.0 APPENDIX.....	VI-31

LIST OF FIGURES	Page No.
Figure 1. Observed Hydraulic Diffusivity ($D_{RH}/D_{100\%}$) as a Function of Relative Humidity (modified from Bazant and Najjar, 1971).....	VI-10
Figure 2: Illustration of Moisture Transport Regimes with Respect to Liquid Saturation (modified from Garrabrants and Kosson 2003).....	VI-10
Figure 3: Permeability Test Apparatus (CRD 1992).....	VI-11
Figure 4: Triaxial Permeability Test Apparatus (CRD 1992).....	VI-12
Figure 5: Steps in the Dynamic Pressurization Method (Scherer 2006).....	VI-13
Figure 6: Critical Pore Radius (i.e., continuous pore diameter) and Threshold Radius from MIP Data (Nokken and Hooton 2006; Nokken and Hooton 2008).....	VI-14
Figure 7: Water Content Profiles Measured using NMR Techniques (Pel, Brocken et al. 1996).....	VI-16
Figure 8: Hydraulic Conductivity of a Saturated Crack as a Function of Aperture.....	VI-18
Figure 9: Effective Unsaturated Hydraulic Conductivity Derived for a Hypothetical Cracked Concrete based on Or and Tuller (2000).	VI-20

LIST OF TABLES

Table 1. Hydraulic Diffusivities of Building Materials (Hall & Hoff 2002).....	VI-8
Table 2. Increase in Cracked Concrete Permeability over Uncracked Materials (Černý & Rovnaníková 2002).	VI-19
Table 3. Selected Parameters for a Hypothetical Cracked Concrete.....	VI-20

LIST OF ABBREVIATIONS AND ACRONYMS

DFM	Discrete Fracture Modeling
DOE	Department of Energy
MIP	Mercury Intrusion Porosimetry
MVG	Mualem-van Genuchten (Model)
NMR	Nuclear Magnetic Resonance
NRC	Nuclear Regulatory Commission
REV	Representative Elemental Volume
RH	Relative Humidity

LIST OF NOMENCLATURE

Roman Characters

- A empirical fitting parameter for hydraulic diffusivity as a function of water content [-]
- b fracture aperture [m]
- B empirical fitting parameter for hydraulic diffusivity as a function of water content [-]
- C chemical potential
- C_y partial pressure [-] of species y in the gas phase (e.g., water)
- d_c characteristic diameter (i.e., threshold or critical diameter) of pores as determined through MIP and the Washburn equation, i.e., the diameter at which pores form a connected network throughout the specimen and accompanied by a spike in the differential pore size distribution curve during the initial mercury intrusion
- $D_{100\%}$ observed moisture diffusivity at 100% relative humidity
- D_{ej} effective water diffusivity of phase j where j , is v for water vapor or a dry air in the gas phase [m^2/s]
- D_θ water or hydraulic diffusivity as a function of water content [m^2/s]
- $D_{\theta,sat}$ saturated hydraulic diffusivity [m^2/s]
- D_{RH} water or hydraulic diffusivity as a function of relative humidity [m^2/s]
- E electrical potential
- F formation factor [-]
- g acceleration due to gravity [$9.8 m/s^2$]
- G conductance [m^2/s]
- G_c critical conductance [m^2/s]
- h total head [m]
- H hydraulic potential [m/m]
- h_c capillary or matric head [m]
- j fluid flux in a single capillary tube as per the Hagen-Poiseuille equation [m^3/s]
- k_{ri} relative permeability factor for phase i , where i is ℓ for liquid or g for gas [-]
- k' intrinsic permeability [m^2]
- K_ℓ hydraulic conductivity [m/s]
- \mathbf{K}_i conductivity tensor [varies] for potential gradient i , where i is hydraulic H , chemical C , , electrical E , or thermal T potential
- \mathbf{K}_ℓ hydraulic conductivity tensor [m/s]
- l length of a capillary cylinder [m] as per the Hagen-Poiseuille equation
- L fracture groove depth [m]
- m van Genuchten model fitting parameter [-]
- M_w molar mass of water [g/mol]
- n van Genuchten model fitting parameter [-]

LIST OF NOMENCLATURE (contd)

Roman Characters (contd)

P_0	saturation vapor pressure [atm]
P_{atm}	atmospheric pressure [atm]
P_A	applied external pressure [Pa]
P_c	capillary pressure [Pa]
P_{cr}	critical pressure defining the transition between flat and curved interfaces [Pa]
P_ℓ	liquid pressure [Pa]
P_g	gas pressure [Pa]
P_p	pressure of the pore fluid [Pa]
P_v	water vapor pressure [Pa]
$q_{\ell \rightarrow v}$	rate of liquid water vaporization per unit volume [$\text{kg} \cdot \text{m}^{-3} \cdot \text{s}^{-1}$]
r	radius of curvature of the liquid-air interface in a capillary pore [m]
r_c	maximum radius of the liquid-vapor interface in a V-shaped groove [m]
R	universal gas constant [$8.314 \text{ m}^3 \cdot \text{Pa} \cdot \text{mol}^{-1} \cdot \text{K}^{-1}$]
RH	relative humidity [%]
RH_c	critical relative humidity [%]
S_e	effective saturation [-]
S_ℓ	saturation of the liquid phase [m^3 liquid-occupied porosity / m^3 total porosity]
S_r	residual saturation of the liquid phase [m^3 liquid-occupied porosity / m^3 total porosity]
t	time [s]
T	absolute temperature [K]
\mathbf{U}	tensor of volumetric water flux through a porous medium [m/s]
\mathbf{U}_i	tensor of volumetric water flux through a porous medium [m/s] for potential gradient i , where i is hydraulic H , chemical C , electrical E , or thermal T potential [varies]
v_i	pore velocity of phase i where i is ℓ for liquid, v for vapor, or a for dry air [m/s]
w/c	water-cement ratio [kg/kg]
x	distance [m]
z	position in the vertical direction [m]

LIST OF NOMENCLATURE (contd)

Greek Characters

- α van Genuchten model fitting parameter [-]
 β empirical fitting parameter for hydraulic diffusivity as a function of relative humidity [-]
 γ empirical fitting parameter for hydraulic diffusivity as a function of relative humidity [-]
 ε_0 initial strain [-]
 ε_∞ residual strain [-]
 ζ fracture groove angle [°]
 η_i dynamic fluid viscosity of phase i where i is ℓ for liquid, g for gas [Pa·s]
 θ liquid water content [m^3 water / m^3 total specimen volume]
 θ_r residual liquid water content [m^3 water / m^3 total specimen volume]
 θ_s saturated liquid water content [m^3 water / m^3 total specimen volume]
 κ intrinsic permeability tensor [m^2]
 λ empirical fitting parameter for hydraulic diffusivity as a function of relative humidity [-]
 ξ empirical fitting parameter for hydraulic diffusivity as a function of relative humidity [-]
 π osmotic suction [Pa]
 ρ_i density of phase i where i is ℓ for liquid, v for water vapor, or a for dry air [kg/m^3]
 σ interfacial surface tension [N/m]
 τ tortuosity of a porous material [m/m]
 ϕ porosity [m^3 pore volume / m^3 sample]
 φ Boltzmann transform [$\text{m}/\text{s}^{1/2}$]
 χ empirical fitting parameter for hydraulic diffusivity as a function of saturation [-]
 Ψ total liquid suction of a porous medium [m]
 Ψ_c capillary potential [m]
 ω empirical fitting parameter for hydraulic diffusivity as a function of relative humidity [-]

MOISTURE TRANSPORT REVIEW

J. R. Arnold and A. C. Garrabrants
Vanderbilt University, School of Engineering
Consortium for Risk Evaluation with Stakeholder Participation, III
Nashville, TN 37235

E. Samson
SIMCO Technology, Inc.
Quebec City, Canada

G. P. Flach and C. A. Langton
Savannah River National Laboratory
Aiken, SC 29808

ABSTRACT

Moisture transport plays a key role in determining how cementitious materials respond to exposure conditions and release contaminants to the external environment. Moisture presence and movement, whether in the form of liquid water and/or water vapor, affect the concentration and transport rates of dissolved and vapor constituents. The fundamentals of moisture transport in cementitious materials are discussed. Various moisture transport formulations and associated properties are summarized with particular emphasis on moisture transport in fractured or otherwise damaged cementitious materials.

1.0 INTRODUCTION

Water acts as both a reaction medium and a transport pathway in a porous material. Thus, moisture transport plays a key role in determining how cementitious materials respond to exposure conditions and release contaminants to the external environment. Specifically, moisture presence and movement, whether in the form of liquid water and/or water vapor, affect the concentration and transport rates of dissolved and vapor constituents. Moisture transport is primarily driven by pressure and gravitational head gradients, but other potentials may influence migration. Local pressure conditions are controlled by capillary suction and vapor-liquid equilibrium in addition to boundary conditions.

The fundamentals of moisture transport in cementitious materials are well understood, and a variety of effective modeling approaches have been advanced for predicting moisture movement. Various moisture transport formulations and associated properties are summarized in this section. Particular emphasis is placed on moisture transport in fractured or otherwise damaged cementitious materials, which are of particular interest to the Cementitious Barriers Partnership (CBP). Physical processes, such as thermal and mechanical cracking, and chemical processes, such as continued hydration, portlandite dissolution, or ettringite and calcite formation, may alter the intrinsic properties of the material such

that the rate of moisture migration is significantly affected. Therefore, defining material properties from initial placement through evolving degradation is essential for the predicting the long-term performance of cementitious materials.

2.0 BACKGROUND

The term *moisture transport* is used to refer to water (H₂O) migration through a porous or fractured medium as both a vapor and a liquid. While both gas and liquid phase moisture transport is discussed, emphasis is placed on liquid water migration. Ingress and release of constituents into and from cementitious waste forms occurs predominately through the liquid phase, making liquid moisture transport more significant than gas-phase migration. However, gas phase transport is important relative to condensation and drying processes in unsaturated materials, whereby water uptake or reaction with other gas-phase constituents such as carbon dioxide or oxygen may occur.

2.1 Morphology and Terminology

The volume fraction of a porous material not occupied by solids is defined as the *total porosity* of the material. While moisture may be present in liquid and/or gas phases throughout the total porosity, only water that is not chemically or physically bound to cement and resides in voids with connection to external boundaries is available for transport. Thus, a distinction is made between *open porosity* and *closed porosity*, the former playing a principal role in moisture transport (Hall & Hoff 2002). Chemically bound water is associated with the cement gel, hydrated mineral phases, and crystalline phases (Černý & Rovnaníková 2002) and is classically considered to be fixed such that it does not participate in moisture transport. The volume occupied by these bound waters is included in the closed porosity. However, bound water may indeed transport through differences in the state of

bound water (Nilsson 2003). Free water is held by surface tension (capillary) forces. Such water can migrate, provided the void space is connected in some manner to an external boundary. The closed or disconnected porosity is often lumped with physical solids in defining the “solid” matrix for analysis purposes. In subsequent discussion, the abbreviated term *porosity* is used with the understanding that open porosity is implied.

From the perspective of long-term performance assessment, cement hydration is also assumed to be practically complete, with respect to moisture transport analysis, such that porosity and associated microstructure are fixed. Characterization of early age porosity and pore structure evolution does not assume complete cement hydration. Likewise, studies dealing with alteration of mature cementitious materials (e.g., some chemical reactions generate water) make assumptions appropriate to the phenomena. Microstructural evolution of cementitious matrices as a function of aging and chemical and structural degradation is presented in a separate chapter.

In cementitious materials, porosity generally takes the form of small-scale interstitial voids or pores between cemented solid grains/aggregates. Void space in the form of cracks or fractures may be present as an initial condition of the material (e.g., thermal and shrinkage cracking) or occur in a number of exposure and damage scenarios (e.g., early-age cracking, sulfate attack, rebar corrosion). While cracking typically has a small impact on void volume, fractures can dramatically affect moisture transport, particularly under saturated or low suction conditions in the case of liquids. Key fracture attributes influencing transport are aperture, crack density, and the degree of connectedness. The term *porous medium* is sometimes reserved for an un-cracked material to distinguish from a *fractured medium*, although both media are porous. Moisture transport in fractured materials is of particular relevance to long-term performance of cement-based materials,

because several degradation scenarios lead to damage in the form of cracks, spalling, etc.

2.2 Mechanisms of Moisture Transport

Moisture transport is driven by gradients of thermodynamic potentials, principally fluid pressure. The transport rate depends on pressure and other gradients, fluid properties, fluid saturation, and the intrinsic permeability of the porous medium. Pressure conditions are influenced by external boundary conditions, and local vapor-liquid thermodynamic equilibrium in the presence of capillary and osmotic suctions.

2.2.1 Flow-Inducing Potentials

In principle, fluid flow can be induced by multiple potential gradients (Bear 1972). Hydraulic head or pressure gradients are the primary driver in most applications. Chemical, electrical and thermal gradients, typically considered of secondary or negligible influence, can also be important to fluid transport.

From the perspective of a porous medium continuum, the overall volumetric water flux \mathbf{U} can be expressed as:

$$\mathbf{U} = -\mathbf{K}_H \Delta H - \mathbf{K}_C \Delta C - \mathbf{K}_E \Delta E - \mathbf{K}_T \Delta T \quad (1)$$

where: H , C , E and T are hydraulic, chemical, electrical and thermal potentials and \mathbf{K}_i is the conductivity tensor for potential gradient i (de Marsily 1986).

The velocity contribution under a hydraulic gradient, i.e., the first term in Eq. (1), is one form of Darcy's Law, and the remaining terms represent chemical, electrical and thermal osmosis respectively. Among the latter effects, chemical osmosis can be significant in cement-based materials. Examples include ice accretion (Erlin & Mather 2005), damage from alkali-aggregate reaction (Gambhir 2004; McArthur & Spalding 2004), and evaporation in the presence of high salt concentrations (Scherer 1999).

In Darcy's Law, the flux of water transporting through a porous media is proportional to the hydraulic gradient by a factor called the hydraulic conductivity:

$$\mathbf{U} = -\mathbf{K}_H \nabla H \quad (2)$$

The hydraulic conductivity can be decomposed into components of permeability and fluid properties while the hydraulic gradient is separated into pressure and elevation contributions yielding:

$$\mathbf{U} = -\frac{\boldsymbol{\kappa}}{\eta_\ell} k_{r\ell} [\nabla P_\ell + \rho_\ell g \nabla z] \quad (3)$$

where: $\boldsymbol{\kappa}$ is the intrinsic permeability tensor, $k_{r\ell}$ is a relative permeability function, η_ℓ is dynamic fluid viscosity, P_ℓ is fluid pressure, $\rho_\ell g$ is specific weight, and z is elevation relative to a reference plane.

The intrinsic permeability is a property only of the porous medium and is not dependent on fluid properties. Relative permeability is a function of the fraction of liquid filled pore volume referred to as *pore saturation*.

With respect to liquid water transport in the presence of a semi-permeable membrane or strong variations in solute concentration, the chemical potential is more conveniently expressed in terms of an osmotic pressure, such that:

$$\mathbf{U} = +\frac{\boldsymbol{\kappa}}{\eta_\ell} k_{r\ell} \nabla \pi \quad (4)$$

where: the sign-reversal reflects the positive valued osmotic suction, π .

The overall volumetric liquid water flux due to hydraulic gradients and (chemical) osmosis is given by:

$$\mathbf{U} = \mathbf{U}_H + \mathbf{U}_\pi = -\frac{\boldsymbol{\kappa}}{\eta_\ell} k_r [\nabla (P_\ell - \pi) + \rho_\ell g \nabla z] \quad (5)$$

Water vapor transport in unfractured materials is driven primarily by pressure and vapor concentration gradients, with elevation gradient considered

insignificant. The volumetric water vapor flux is typically expressed as an advective flux, from pressure-driven bulk gas flow, plus a diffusive flux relative to the mean flow due to a concentration gradient.

2.2.2 Equilibrium Pressure Conditions

Locally, liquid pressure is coupled to equilibrium vapor pressure through pore structure, water content relative to porosity, and solute concentration(s). Total liquid suction (negative pressure; positive-valued), also known as the *free energy state* of pore water, is the sum of matric and osmotic suctions (Fredlund & Rahardjo 1993; Dao, Morris & Dux 2008):

$$\psi = (P_g - P_\ell) + \pi = \psi_c + \pi \quad (6)$$

where: P_g is gas pressure, P_ℓ is liquid pressure, and ψ_c is matric or capillary suction.

Pore structure, water content, and porosity influence liquid pressure through the matric suction, while the osmotic suction is controlled by solute concentrations. Total suction is closely related to chemical potential.

Total suction is related to vapor pressure through the equilibrium thermodynamic relationship (Richards 1965; Fredlund & Rahardjo 1993):

$$\psi = -\frac{RT}{gM_w} \ln \frac{P_v}{P_0} \quad (7)$$

where: ψ is total liquid suction, R is the universal (molar) gas constant [$\text{m}^3 \cdot \text{Pa} \cdot \text{mol}^{-1} \cdot \text{K}^{-1}$], g is acceleration due to gravity [m/s^2], M_w is molar mass of water [kg/mol], T is absolute temperature [K], P_0 is vapor pressure at saturation [P_v], and P_v is water vapor pressure [Pa].

In light of this expression, water vapor pressure can be viewed as a *master variable* defining the pressure state of both the gas and liquid phases (Hall & Hoff 2002).

2.3 Modeling Formulations

A number of approaches have been devised for describing water transport through porous media. The vast majority involve using macroscopic formulations derived from volume averaging over a Representative Elementary Volume (REV; Bear 1972) or ensemble averaging concepts (Bear & Buchlin 1991). These approaches enable a continuum treatment of porous medium properties and introduce the concept of fluid saturation. *Fluid saturation* is the average presence of the fluid phase within the REV; or the probability of occurrence across an ensemble of realizations.

Fractures within a porous medium can be addressed using continuum or discrete fracture models. Continuum fractured media formulations include: 1) the single-continuum effective property approach, whereby the original porous medium properties are modified to capture the combined effects of matrix and fracture transport, and 2) dual-porosity/permeability models, which utilize a dual-continuum concept whereby water transport occurs in overlapping matrix and fracture volumes. Discrete fracture models explicitly simulate flow through individual fractures while preserving the key attributes of the fracture geometry such as aperture, spacing, asperity, and connectivity.

Pore scale models, although less commonly used, are valuable for investigating pore scale phenomena, such as chemical reactions and crack initiation and propagation within the cement-based material microstructure. Other models of potential interest include lattice-Boltzmann models.

3.0 MOISTURE TRANSPORT IN POROUS MEDIA

3.1 Transport Equations

Mainguy (2001) expressed the mass balance equations for the two-phase, three-component (liquid water, dry air and water vapor) water transport system as:

Liquid

$$\frac{\partial}{\partial t}(\phi S_\ell \rho_\ell) = -\nabla(\phi S_\ell \rho_\ell v_\ell) - q_{\ell \rightarrow v} \quad (8)$$

Water Vapor

$$\begin{aligned} \frac{\partial}{\partial t}(\phi(1-S_\ell)\rho_v) = \\ -\nabla(\phi(1-S_\ell)\rho_v v_v) + q_{\ell \rightarrow v} \end{aligned} \quad (9)$$

Dry Air

$$\frac{\partial}{\partial t}(\phi(1-S_\ell)\rho_a) = -\nabla(\phi(1-S_\ell)\rho_a v_a) \quad (10)$$

where: ϕ is porosity, ρ_i is density of phase (e.g., where i is ℓ for liquid, v for vapor, or a for dry air), S_ℓ is liquid saturation, v_i is velocity of phase i , and $q_{\ell \rightarrow v}$ is the rate of liquid water vaporization per unit volume.

Considering hydraulic and osmotic potentials for liquid flow, the liquid phase Darcy velocity is defined by (5):

$$\phi v_\ell = -\frac{\mathbf{K}}{\eta_\ell} k_{r\ell} \langle S_\ell \rangle [\nabla(P_\ell - \pi) + \rho_\ell g \nabla z] \quad (11)$$

where: the saturation dependence of relative permeability is explicitly denoted as $k_{r\ell} \langle S_\ell \rangle$.

Under these conditions, the gas phase velocity is defined by:

$$\phi v_g = -\frac{\mathbf{K}}{\eta_g} k_{rg} \langle S_\ell \rangle \nabla P_g \quad (12)$$

The water vapor and dry air mass fluxes can then be expressed as the sum of advective and diffusive components as:

$$\begin{aligned} \phi \rho_j v_j = \phi \rho_j v_g \\ - D_{ej} \langle S_\ell \rangle \phi (1-S_\ell) \nabla \rho_j \end{aligned} \quad (13)$$

where: the subscript j indicates air or water vapor components, and $D_{ej} \langle S_\ell \rangle$ is a saturation-dependent effective diffusion coefficient accounting for tortuosity effects.

Several moisture transport models have been developed for various applications using this approach (Šelih, Sousa & Bremner 1996; Gawin, Pesavento & Schrefler 2006; Mainguy, Coussy & Baroghel-Bouny 2001) to describe isothermal drying test results in cementitious materials using the expression:

$$\begin{aligned} \phi_g \rho_j v_j = \phi_g \rho_j v_g \\ - \rho_j \frac{D_j}{C_y} f \langle S_\ell, \phi \rangle \nabla C_y \end{aligned} \quad (14)$$

where: D_j is the diffusion coefficient of component j (e.g., v or a for water vapor or dry air in the gas phase), $f \langle S_\ell, \phi \rangle$ is the resistance factor accounting for both tortuosity effects ($D_{ej} = D_j f$) and the effective area for diffusion and C_y is the partial pressure of species y (e.g., water).

The general multiphase moisture transport equation set is commonly simplified by: 1) neglecting osmotic effects, bulk gas phase transport, and evaporation, 2) assuming constant liquid properties, and 3) taking the gas pressure as uniformly equal to atmospheric pressure. Then the liquid mass balance Eq. (8) and Darcy's Law Eq. (11) can be combined to yield a form of the Richards Equation (1931):

$$\begin{aligned} \frac{\partial \theta}{\partial t} = \nabla \left[\mathbf{K}_\ell k_{r\ell} \langle \theta \rangle \nabla \left(\frac{-\psi_c \langle \theta \rangle}{\rho_{\ell g}} + z \right) \right] \\ = \nabla \left[\mathbf{K}_\ell k_{r\ell} \langle \theta \rangle \nabla h \right] \end{aligned} \quad (15)$$

where: $\theta = \phi S_\ell$ is water content, $\mathbf{K}_\ell = \kappa \rho_\ell g / \eta_\ell$ is hydraulic conductivity tensor, $\kappa_{r\ell}(\theta)$ is relative permeability now expressed as a function of water content, $\psi_c(\theta) / \rho_\ell g$ is matric (capillary) suction head, and h is total head.

The nonlinear relative permeability ($K_{r\ell}(\theta)$) and water retention ($\psi_c(\theta) / \rho_\ell g$) functions must be empirically defined to complete the formulation. Richards equation may not be accurate for cases where the external relative humidity is less than 100%, such that evaporation is important.

Further simplification can be achieved by neglecting gravity effects if present and assuming a homogeneous material, conditions often valid in cementitious material applications. By viewing matric suction as a function of water content and using the chain rule on the right hand side of Eq. (15), the (positive-valued) *water* or *hydraulic diffusivity* parameter can be defined as:

$$\begin{aligned} \mathbf{D}_\theta(\theta) &= \mathbf{K}_\ell k_{r\ell}(\theta) \frac{d(-\psi_c / \rho_\ell g)}{d\theta} \\ &= -\mathbf{K}_\ell k_{r\ell}(\theta) \frac{dh_c}{d\theta} \end{aligned} \quad (16)$$

where: h_c is matric (capillary) suction head.

With this definition, Eq. (15) can then be simplified as:

$$\frac{\partial \theta}{\partial t} = \nabla \left[\mathbf{D}_\theta(\theta) \nabla \theta \right] \quad (17)$$

The nonlinear water diffusivity is normally observed directly from measurements, rather than computed using the above relation, in a similar manner to water retention and relative permeability functions. The water diffusivity formulation is convenient because three material properties (saturated hydraulic conductivity, relative permeability, and water retention) are replaced by a single empirical function. Similar equations using relative humidity as the dependent variable have also been derived (Xi et al. 1994).

3.2 Model Parameters

The material property needs associated with the two simplified moisture transport formulations differ. Richards Equation (15) requires hydraulic conductivity ($\mathbf{K}_\ell = \kappa \rho_\ell g / \eta_\ell$), relative permeability ($k_{r\ell}(\theta)$), and water retention functions ($\psi_c(\theta) / \rho_\ell g$), while Eq. (17) requires only a water diffusivity function ($\mathbf{D}_\theta(\theta)$). The relative permeability, water retention, and water diffusivity functions are referred to as *characteristic curves* of the porous medium (Webb 2006). Although shown as a function of water content (θ), the moisture characteristic curves may also be expressed as functions of saturation through the relationship:

$$\theta = \phi S_\ell \quad (18)$$

These parameters are empirically determined through experimentation and generally exhibit hysteresis, leading to separate wetting/adsorption and drying/desorption curves.

The appendix lists the properties needed to define the physical state of a porous medium. These include the fluid and porous-medium properties related to moisture transport encountered in this chapter and, for completeness, other physical and material properties related to solute transport and leaching processes.

3.2.1 Relative Permeability as a Function of Saturation

Many closed form expressions have been proposed for representing water retention and relative permeability (e.g., Brooks and Corey 1964); however, the Mualem-van Genuchten (MVG) model (Mualem 1976; van Genuchten 1980) is the most widely used. The MVG model defines an effective saturation (S_e) as:

$$S_e = \frac{S - S_r}{1 - S_r} = \frac{\theta - \theta_r}{\theta_s - \theta_r} \quad (19)$$

where: S_e is the effective saturation and the subscripts r and s refer to the residual and saturated water conditions, respectively.

The effective saturation and relative permeability are then expressed as:

$$S_e = \left[\frac{1}{1 + (\alpha h_c)^n} \right]^m \quad (20)$$

$$k_r \langle S_e \rangle = S_e^{1/2} \left[1 - \left(1 - S_e^{1/m} \right)^m \right]^2 \quad (21)$$

where: it is often assumed that $m = 1 - 1/n$.

Thus, the MVG model contains two empirical parameters, n and α . In these expressions, $h_c = \psi_c / \rho_\ell g$ is matric (capillary) suction head.

Although developed in the context of unsaturated soils, the MVG model has been validated for cement concretes (Savage & Janssen 1997; Wardeh & Perrin 2006). The MVG model equations and the input parameters of porosity and moisture desorption curves have been utilized to make indirect measurements of the intrinsic permeability of cementitious specimens (Baroghel-Bouny 2007a). Application of the MVG model in this manner avoids the difficulty in obtaining direct measurements of unsaturated conductivity. However, even saturated permeability can be difficult to determine experimentally due to the relatively low porosity of cementitious materials. Typically, in order to induce flow, large external pressures must be applied to a surface which could potentially result in microstructural damage (Olson, Neubauer & Jennings 1997; Feldman 1984).

If total potential ψ is assumed to be a function of water content θ_ℓ then the change in water content with time may be expressed as a function of only the water content gradient by embedding the value of $K\langle\theta\rangle$ in the hydraulic diffusivity coefficient $D_\theta\langle\theta\rangle$ [m^2/s] as shown in Eq. (16).

The term “diffusivity” was ascribed to water migration because one-dimensional moisture migration is defined by a second order differential equation, analogous to Fick’s second law of diffusion

describing Brownian motion. This nomenclature should be used with caution as the migration of moisture in this instance is due to the chemical, electrical and thermal potentials described above. For clarity, $D_\theta\langle\theta\rangle$ is referred to as water diffusivity or hydraulic diffusivity.

3.2.2 Hydraulic Diffusivity as a Function of Water Content

Although the Mualem-van Genuchten model can be recast in terms of the hydraulic diffusivity parameter (van Genuchten 1980), simpler expressions to parameterize Eq. (17) are typically used for cementitious materials (Hall & Hoff 2002). A common empirical relationship relating 1-D hydraulic diffusivity to water content is:

$$D_\theta = A \exp(B\theta) \quad (22)$$

where: A and B are constants (Hall & Hoff 2002; Mensi, Acker & Attolou 1988).

Table 1 lists hydraulic diffusivity parameter values D_θ for various building materials which may be considered analogs to some cementitious barrier materials.

A non-destructive means of experimentally determining $D_\theta\langle\theta\rangle$ was first reported in 1979 (Gummerson et al. 1979). The method involves measuring time-dependent moisture profiles of one-dimensional water uptake into an initially dry mortar bar via nuclear magnetic resonance (NMR) spectroscopy, a technique which detects the interaction of magnetic moments of nuclei with quantum spin state of +1/2 (including hydrogen) and an applied external magnetic field (Blümich 2000). Neutron radiography has also been successfully employed to determine the hydraulic diffusivity in a similar manner (Pel et al. 1993; Cnudde et al. 2008). However, air blockages which are common in one-dimensional uptake experiments on initially dry samples, may lead to complications with data interpretation.

Table 1. Hydraulic Diffusivities of Building Materials (Hall & Hoff 2002)

Material	Diffusivity	
	$D_{\theta} D_{wsat} [m^2/s]$	$(\theta_3 - \theta_r)B$
Lepine limestone	6.3×10^{-9}	4.9
Cleris limestone	3.2×10^{-9}	6.4
St. Maximin fine limestone	1.3×10^{-8}	5.6
Gres de Vosges sandstone	2.4×10^{-9}	5.0
Clay brick ceramic, moulded	3.4×10^{-9}	8.3
Clay brick ceramic, extruded	2.2×10^{-9}	6.3
Sand-lime brick	7.9×10^{-11}	8.4
1:5 cement:sand mortar	9.5×10^{-10}	8.0
1:3:12 cement:lime:sand mortar	5.7×10^{-8}	6.6

Values of the hydraulic diffusivity $D_{\theta}(\theta)$ may be well fit with exponential equations (Hazrati et al. 2002; Leech, Lockington & Dux 2003; Pel et al. 1998). Some researchers have found sufficient agreement using power law approximations of the form:

$$D_{\theta}(\theta) = D_{\theta,sat} \theta^{\chi} \quad (23)$$

where: $D_{\theta,sat}$ is the hydraulic diffusivity at full saturation and χ is a constant.

However, at least one study suggests that an exponential fit might be a better approximation than power law expressions (Hall & Hoff 2002; Lockington, Parlange & Dux 1999). Neither Eq. (20) nor Eq. (21) has a strong theoretical basis, but both expressions have been found useful for describing moisture transport in cementitious materials (Hall & Hoff 2002).

Boltzman Transform Approach

A closed form solution for the hydraulic conductivity parameter shown in the partial differential equation Eq. (16) may be found through the Boltzman transformation:

$$\varphi = xt^{-1/2} \quad (24)$$

The resulting partial differential equation takes the form:

$$-\frac{\varphi}{2} \frac{d\theta}{d\varphi} = \frac{d}{d\varphi} \left(D_{\theta} \frac{d\theta}{d\varphi} \right) \quad (25)$$

Setting the conditions that $\theta = \theta_S$ at $\varphi = 0$ and $\theta = \theta_r$ as $\varphi \rightarrow \infty$, the closed form solution is given by (Hall & Hoff 2002):

$$x(\theta, t) = \phi(\theta) t^{1/2} \quad (26)$$

Eq. (26) demonstrates that plotting water content as a function of φ will result in a single master curve, and by dividing the master curve into small increments from the residual water content θ_r to any water content θ_x , hydraulic diffusivity may be determined via the Matano method as (Hall & Hoff 2002; Matano 1932–33):

$$D_{\theta}(\theta_x) = \frac{1}{\left(\frac{d\theta}{d\varphi} \right)_{\theta_x}} - \frac{1}{2} \int_{\theta_r}^{\theta_x} \varphi d\theta \quad (27)$$

3.2.3 Hydraulic Diffusivity as a Function of Relative Humidity

A similar expression of moisture transport shown in Eq. (17) has also been derived using relative humidity RH as the dependent variable (Xi et al.

1994). This approach assumes that the driving force can be expressed as: $U = -D_{RH} \nabla RH$ where D_{RH} is hydraulic diffusivity as a function of RH . In that case, Eq (17) can be written as (Bazant & Najjar 1971; Xi et al. 1994; Garrabrants & Kosson 2003):

$$\frac{\partial \theta}{\partial RH} \frac{\partial RH}{\partial t} = \nabla (D_{RH} \nabla RH) \quad (28)$$

where: $\partial \theta / \partial RH$ represents the water content as a function of relative humidity.

In practice, this relationship exhibits hysteresis, that is, the function is distinct depending on whether the specimen adsorption or desorption is measured. However, due to the shape of the adsorption and desorption curves being nearly the same (Hagymassy et al. 1972), use of the term $\partial \theta / \partial RH$ is consistent whether measured from wetting or drying experiments.

Inference of hydraulic diffusivity from these relatively simple water sorption/desorption experiments has proven successful although somewhat sensitive to experimental conditions (Ketelaars et al. 1995; Garbalinska 2006; Anderberg & Wadsö 2008). Experiments of this type typically involve measurement of mass change over short time intervals and can be fit to analytical solutions of diffusivity (Crank 1975) or to empirical forms. An empirical expression was presented by Xi et al 1994) as:

$$D_{RH} = \lambda + \beta \left(1 - 2^{-10\gamma(RH-1)} \right) \quad (29)$$

where: λ , β and γ are parameters that need to be determined experimentally.

Two Regime Model

The hydraulic diffusivity expression used by Garrabrants and Kosson (2003) was derived from

the work of Bazant and Najjar (1971) in which the function is described as “an S-shaped curve” with the general expression:

$$D_{RH} = D_{100\%} \left[\zeta + \frac{1-\zeta}{1 + \left(\frac{1-RH}{1-RH_c} \right)^\omega} \right] \quad (30)$$

where: $D_{100\%}$ is the observed moisture diffusivity at 100% relative humidity and ζ , ω , and RH_c are fitting parameters.

Bazant and Najjar described the ratio of $D/D_{100\%}$ as an “S-shaped” curve where ζ is the ratio of $D_{0\%}/D_{100\%}$, ω represents the spread in the drop of the S-shaped curve, and RH_c is a critical relative humidity corresponding to the center of the drop in curve (Figure 1).

Garrabrants and Kosson interpreted the dependence of the hydraulic diffusivity on water saturation (or relative humidity) with respect to the evolution of continuous liquid and gas phases during the drying process (Figure 2). The critical phases of the drying process include:

- **Funicular Drying (Fully Saturated to Capillary Saturation):** RH at the bulk material surface is 100% and evaporation away from surface is driven by the relative humidity gradient between the surface and ambient conditions. During this funicular drying regime, bulk phase movement occurs in response to pressure gradients within the porous network and the liquid phase is considered to be continuous while the gas phase is discontinuous at $RH=100\%$.
- **Transition Zone Drying (Capillary Saturation to Insular Saturation):** At capillary saturation, both liquid and gas phases are continuous and the observed hydraulic diffusivity is a combination of bulk liquid movement and vapor transport. During the transition zone drying regime, the ratio of $D_{RH}/D_{100\%}$ drops toward the value of ζ .

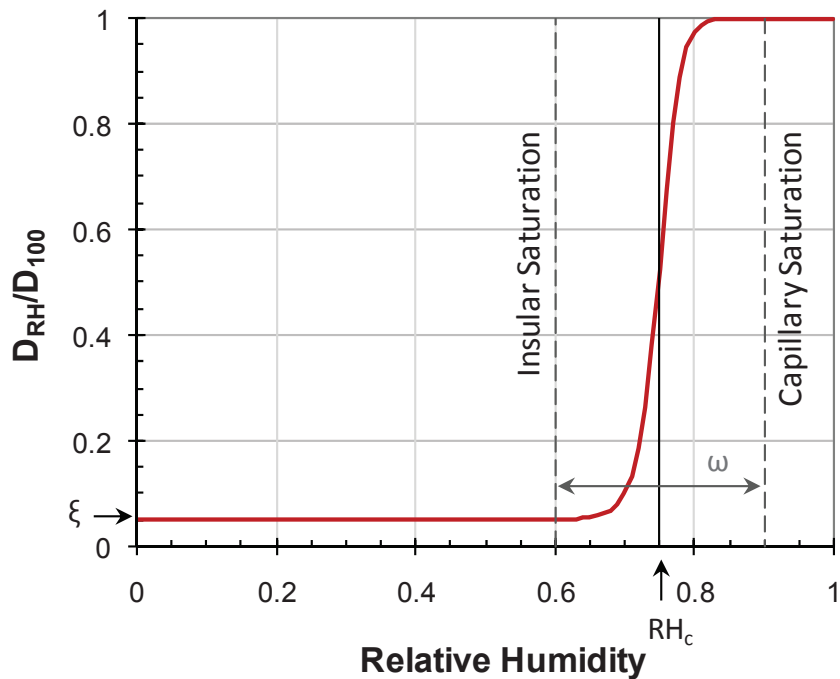


Figure 1. Observed Hydraulic Diffusivity ($D_{RH}/D_{100\%}$) as a Function of Relative Humidity (modified from Bazant and Najjar, 1971)

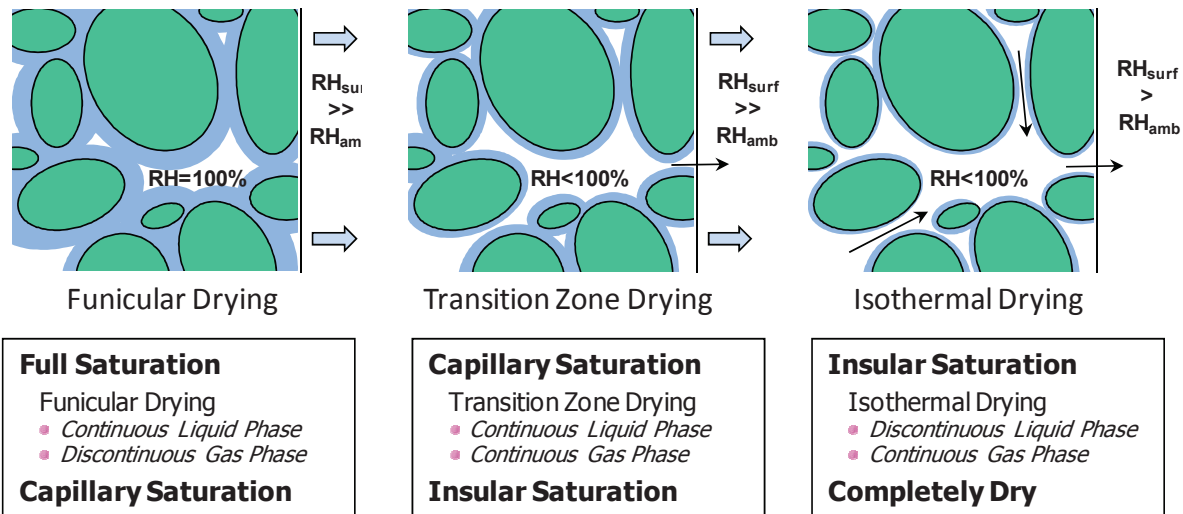


Figure 2: Illustration of Moisture Transport Regimes with Respect to Liquid Saturation (modified from Garrabrants and Kosson 2003)

- Isothermal Drying (Insular Saturation to Completely Dry):** At the point of insular saturation, liquid phase becomes discontinuous and moisture transport is dominated by the diffusion of water vapor in the continuous gas phase. The water content is given as a function of internal RH through the vapor-liquid isotherm and this phase of the drying process is referred to as the isothermal drying regime. However, the theoretical construct of a “completely dry” cementitious matrix is not realistic, even at very low ambient relative humidity, due to existence of bound water in the matrix.

3.3 Selected Model Parameter Measurements

Accurate simulation of moisture transport using either the Richards equation (15) or the hydraulic diffusion equation requires measurement of key moisture parameters. For the Richards equation, these parameters include the hydraulic conductivity,

relative permeability, and water retention functions while a water diffusivity function and vapor-liquid isotherm may be required for the hydraulic diffusion equation. Several direct and indirect measurement methods are available.

3.3.1 Saturated Hydraulic Conductivity (Permeability)

Direct Permeability Methods: The direct estimation of cementitious material permeability is based on Darcy’s law shown in Eq. (2) and consists of exposing a saturated material sample to a constant 1-D pressure gradient with measurement of the water flow across the sample. The 1-D water transport is enforced by coating the side surface of the sample with epoxy or a similar sealant. Upon reaching steady-state, the permeability is calculated from the ratio of the flow over the applied pressure gradient. This methodology is used in the CRD-C 48-92 *Standard Test Method for Water Permeability of Concrete* (CRD 1992a) and the experimental setup is illustrated in Figure 3.

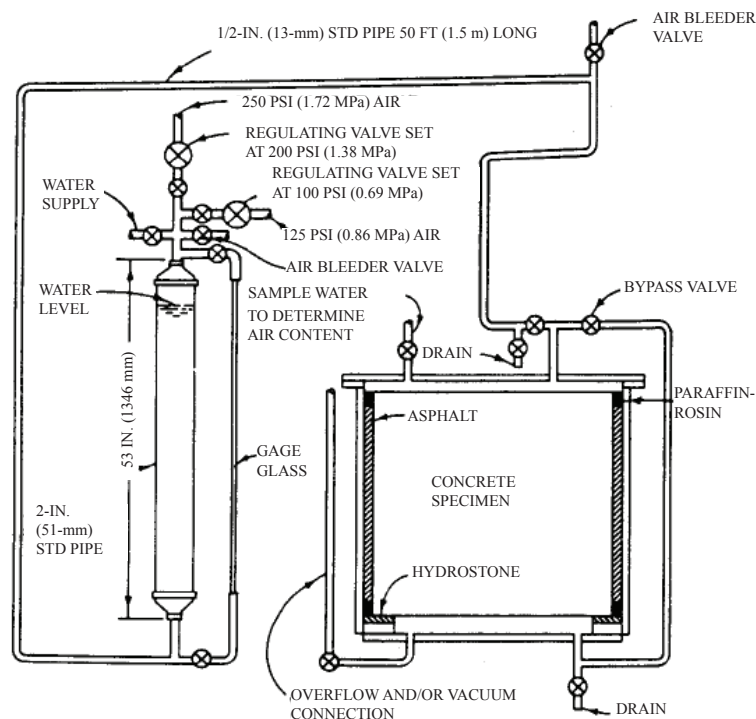


Figure 3: Permeability Test Apparatus (CRD 1992)

Although the principle is very simple, this method has been hampered by the material itself. The highly tortuous and narrow pore network of cementitious materials translates into very low permeability values and, consequently, high pressures are needed to generate a measurable and stable flow. High pressures can lead to leakages around the sample (Hope & Malhotra 1984). In addition, the surface of the sample must be dried in order to apply most sealants or coatings, which may affect the permeability estimation (Scherer, Valenza & Simmons 2007). Because of these experimental problems, high variability in permeability values have been reported (El-Dieb & Hooton 1995). Improvements to the basic setup have been proposed in the literature (Hope & Malhotra 1984; Hearn & Mills 1991), but, overall, the method is not well adapted to high quality materials due to the high pressure needed to maintain constant water flows (Nokken & Hooton 2008).

An alternate method for measuring permeability was proposed based on the use of a triaxial test (CRD 1992b). The basic principle is the same as the previous method except that lateral pressure is applied on a rubber sleeve surrounding the entire sample to prevent leakages (see Figure 4).

Variations on this setup have been proposed in the literature (e.g., (El-Dieb & Hooton 1994b)). Test results with the triaxial procedure showed less variability than with the previous method, even for high quality materials (El-Dieb & Hooton 1995). Despite these improvements, the triaxial method is rarely used (Nokken & Hooton 2008).

Indirect Permeability Methods: The technical difficulties associated with the direct methods have led to the development of indirect methods, where the experimental conditions are easier to control. On the other hand, these methods often are accompanied by theory that is more complex than the simple theory of Darcy's law.

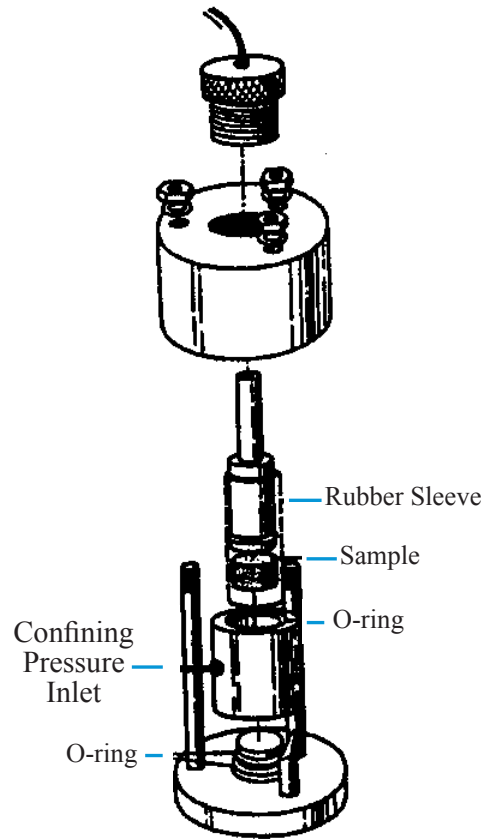


Figure 4: Triaxial Permeability Test Apparatus (CRD 1992)

The Dynamic Pressurization Technique (Scherer 2006) is illustrated in Figure 5. A saturated material is immersed in a vessel filled with water with the initial pressure of the water in the vessel (P_v) and in the pore fluid (P_p) is equal to the atmospheric pressure (P_{atm}). At the start of the experiment ($t = 0^+$), a pressure jump (P_A) is applied to the liquid in the vessel and maintained for the remainder of the test. The applied pressure contracts the sample (ϵ_0), in part, because the initial pore pressure is less than the applied pressure. Over time, the pore fluid reaches the same pressure as the vessel pressure and the material contraction relaxes somewhat. When equilibrium is reached, the sample still exhibits a

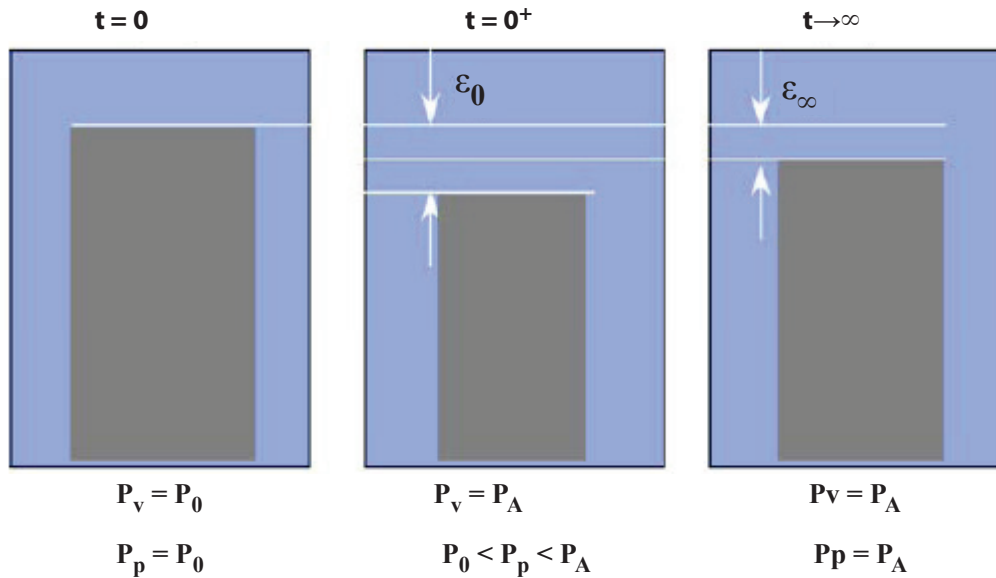


Figure 5: Steps in the Dynamic Pressurization Method (Scherer 2006)

contraction (ϵ_∞) that is less than the initial contraction (ϵ_0). The relaxation time is a function of the permeability of the material which can be calculated from the dynamic pressurization technique theory (Scherer 2006).

Grasley et al. (2007) have described the application of the dynamic pressurization technique to hydrated cement pastes (w/c of 0.4, 0.5, 0.6) and concrete samples (w/c of 0.5). The method showed good repeatability, but the results were not compared to permeability values obtained with direct methods. This technique is best suited to material with low permeability because the rapid relaxation times of highly permeable materials renders this technique difficult (Jones & Grasley 2009).

A related method called *Beam-Bending Method* has been developed (Scherer, Valenza & Simmons 2007; Vichit-Vadakan & Scherer 2002). The method consists of applying a three-point bending load to a beam-shaped sample immersed in water in order to maintain a fixed deflection. The deformation induced by the load creates pressure gradients in the material

that are not in equilibrium with the pressure in the surrounding fluid. As the pore pressure equilibrates, the force required to sustain a fixed deflection decreases, and the kinetics of relaxation of the force can be analyzed to obtain the permeability (Scherer, Valenza & Simmons 2007).

Comparisons between permeability values of hydrated cement pastes obtained with the beam-bending and dynamic pressurization techniques showed good agreement between the methods (Grasley et al. 2007).

Another indirect method to estimate the permeability of cementitious materials is based on the pore size distribution and the *Katz-Thompson permeability theory* (Katz & Thompson 1986; Garboczi 1990; Scherer, Valenza & Simmons 2007). The Katz-Thompson theory assumes fluid transport through pores will not be possible unless pores intersect, forming a connected network which spans the specimen length. The theory states:

$$k' = \frac{1}{226} d_c^2 \frac{\phi}{\tau} \quad (31)$$

where: k' is the intrinsic permeability, d_c^2 is the critical pore diameter, ϕ is the porosity and τ is the tortuosity.

The ratio $1/226$ is not empirical, but is a calculated value resulting from the cylindrical pore assumption and the theory of mercury intrusion porosimetry (MIP). The ratio τ/ϕ is called the formation factor F which can be estimated from bulk and pore solution conductivity analysis (Snyder & Marchand 2001). The tortuosity can be estimated on the basis of migration test results (Samson et al. 2008). The critical pore diameter d_c can be estimated from MIP results, where successive volumes of mercury dV are forced into the material under pressure increments dP .

3.3.2 Porosity and Pore Size Distribution Measurements

Mercury intrusion porosimetry (MIP) has frequently been employed to measure the distribution of pore sizes from cementitious samples. To be precise, the result obtained through MIP is not a pore size distribution but

rather a pore-throat size distribution (Diamond 2000). The inflection point of the cumulative-intruded-volume pore size distribution curve (corresponding to the maximum of the differential-intruded-volume curve) denotes an equivalent pore diameter which accounts for the largest volume contribution to the pore space (Figure 6).

The parameter d_c corresponds to the inflection point in the curve relating the intruded mercury volume to the pore radius, as shown in Figure 6. Thus, a characteristic diameter d_c [m] may be defined which is proportional to the intrusion pressure and which accounts for the greatest overall volume contribution to the porosity. The importance of d_c follows from the idea that, in a system of randomly distributed conductances, the cumulative conductance is influenced much more strongly by conductances $G \geq G_c$. The characteristic conductance G_c represents the largest conductance at which all conductances form an infinite, connected path and thus, corresponds to the diameter d_c in the case of MIP (Katz & Thompson 1986).

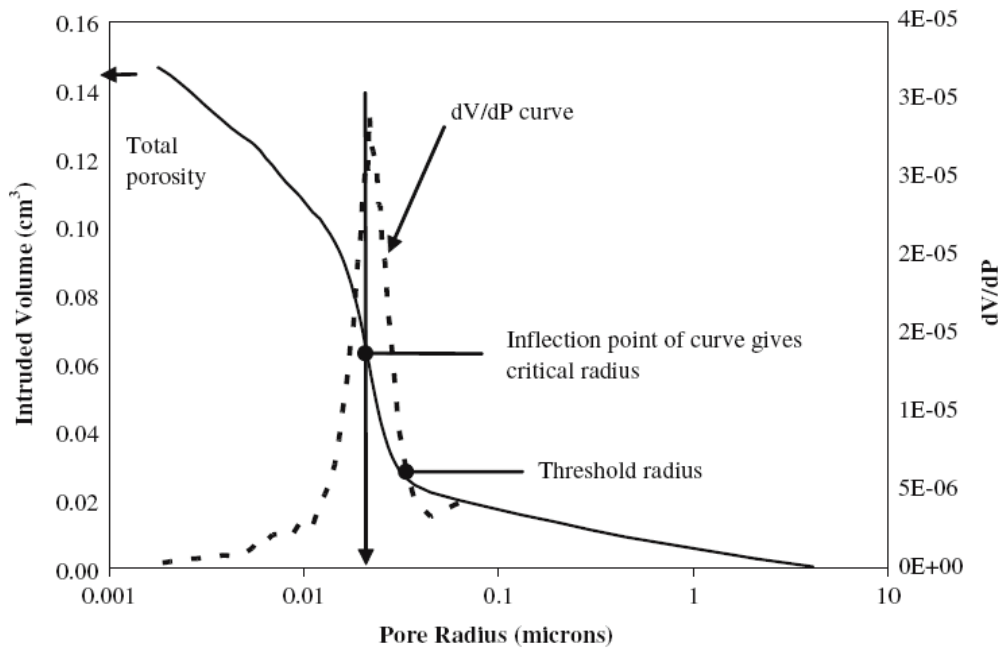


Figure 6: Critical Pore Radius (i.e., continuous pore diameter) and Threshold Radius from MIP Data (Nokken and Hooton 2006; Nokken and Hooton 2008)

The applicability of Eq. (31) to cementitious materials has been discussed in many references. Test results obtained on hydrated cement pastes have validated the relationship (Nokken & Hooton 2008; Christensen, Mason & Jennings 1996). However, the Katz-Thompson theory has proven insufficient for predicting permeability of cement paste and concrete (El-Dieb & Hooton 1994a). Similarly, the Katz-Thompson model was demonstrated to consistently under-predict permeability values of concretes by two orders of magnitude (Tumidajski & Lin 1998). Halamickova (Halamickova et al. 1995) obtained good results with the Katz-Thompson model for hydrated cement pastes made at w/c 0.5, but proposed to modify the constant to 1/180 for w/c 0.4 pastes. Cui and Cahyadi (2001) argue that the Katz-Thompson model as shown cannot be applied to cementitious materials because the pore structure is a combination of two distinctive pore classes (i.e., fine gel pores and coarser capillary pores) and significantly improved the accuracy by modifying the equation to account for transport through gel pores using general effective medium theory (Cui & Cahyadi 2001).

Another parameter obtained from the MIP curve and used to predict permeability is the threshold diameter, that is the diameter corresponding to the lowest pressure at which mercury is able to begin invading the interior of the specimen through a connected, or percolating path, filling larger but previously disconnected pores termed “ink-bottle” pores (Hall & Hoff 2002; Moro & Bohni 2002). Thus the threshold diameter is typically defined somewhat arbitrarily as the diameter corresponding to the intrusion pressure where mercury first begins to invade the specimen in significant quantity (Nokken & Hooton 2006).

3.3.3 Measurement of Hydraulic Diffusivity

Test method ASTM E96-90 (ASTM E96 2005) is a so-called “cup test” method that is used to determine

hydraulic diffusivity by placing a cementitious slab in a sealed apparatus such that two opposing sides of the slab are exposed to different relative humidity conditions controlled by salt solutions. As relative humidity equilibrates via moisture movement through the sample, the mass of the salt-solution in one chamber is monitored until a steady flow of vapor is reached. Hydraulic diffusivity can then be calculated from these steady flow mass change measurements (Mosquera et al. 2006; Baroghel-Bouny 2007b).

An alternate methodology, based on drying an initially saturated sample at 50% relative humidity, has been used to estimate the A and B parameters of the exponential expression shown in Eq. (22) for the hydraulic diffusivity (Samson et al. 2008). Two series of samples with different thicknesses (i.e., 1-cm and 5-cm thick) are dried at 50% RH until the masses of the thinner samples have stabilized. The drying step can take up to three months for high performance concretes. The stabilized mass of the thinner samples provides the equilibrium water content at 50% RH if the porosity of the material is known. The thicker drying series is terminated when the mass of the thinner samples is stable. Using the equilibrium value obtained for the thin samples series, a numerical algorithm solves Richards equation and adjusts A and B in Eq. (22) to fit the mass loss curves of the 5-cm series. Results show that a value of $B = 80$ can be used for most concrete mixtures.

The ingress of absorbed water into oven-dried samples of construction materials has been investigated using NMR techniques (Pel 1996) and X-ray tomography (Carmeliet 2004). Figure 7 shows the moisture content profiles for a material using NMR (Pel 1996). With both techniques, the profiles at different time intervals were analyzed using the Boltzmann transformation of Richards equation to yield the liquid water diffusivity.

Such approaches are influenced by problems in sample preparation, analytical techniques and

interpretation of the acquired data. The method also relies on drying the samples before water absorption takes place. Marsh et al. (1983) argued that the process of oven-drying concrete samples induces microcracks that can affect the water transport characteristics. Coarse aggregates, air voids, and even sand grains weaken the signal and prevent reliable analysis. Marsh et al. noted that the Boltzman transform, and in general scaling uptake to $t^{1/2}$, is strictly limited for one-dimensional cases and anomalies from $t^{1/2}$ scaling may result from trapped air during uptake. In general, these techniques are limited to mostly homogeneous hydrated cement paste.

3.4 Qualitative Tests

Other test methods exist to assess the moisture transport characteristics of cementitious materials, such as ISO12572 and ASTM C1585. These test methods allow qualitative comparisons between

materials, but do not provide a direct estimation of transport properties.

In the ISO12572 procedure, entitled *Hygrothermal Performance of Building Materials and Products*, cylindrical samples are exposed to humidity gradients. One face is maintained close to water, thus creating a high humidity boundary condition. The other face is exposed to a lower humidity environment. The humidity gradient drives water through the sample. The mass of the set-up is measured until it is stable. The test provides the steady-state moisture flux across the sample. The method is similar to the ASTM E96 *Standard Test Methods for Water Vapor Transmission of Materials* which can be applied to any porous materials, including concrete.

The procedure ASTM C1585 *Standard Test Method for Measurement of Rate of Absorption of Water by Hydraulic-Cement Concretes* consists of exposing a pre-dried cylindrical sample to water vapor at 50-70% RH causing the cementitious material to absorb water. During absorption, mass is recorded on a regular basis and the experimental data is expressed in terms of the volume of water absorbed per unit surface area (e.g., mm^3/mm^2). Data are plotted against the square root of time and the curve usually shows two linear segments, respectively called initial and secondary absorption. The slope of the initial absorption is called the sorptivity and can be used to compare the absorption of different cementitious materials.

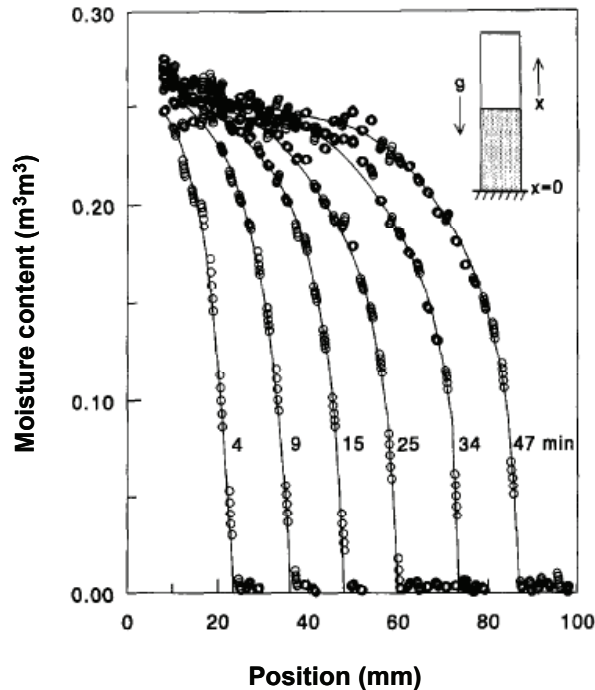


Figure 7: Water Content Profiles Measured using NMR Techniques (Pel, Brocken et al. 1996)

4.0 MOISTURE TRANSPORT THROUGH FRACTURED MEDIA

Although undesirable, cementitious materials may become fractured due to various design, placement, and exposure/degradation conditions. Fractures generally enhance water (and solute) transport under saturated and film flow conditions. The extent depends on saturation conditions and fracture aperture, spacing, asperity, and connectivity. Thus,

moisture transport in fractured media is of particular relevance to the performance of damaged engineered cementitious barriers.

4.1 Role of Fractures in Moisture Transport

Under saturated conditions, cracks typically dominate liquid moisture flow and solute transport. Under unsaturated conditions and sufficient matric suction, fractures become relatively inactive in transporting water and dissolved species, because they are effectively dewatered and may also form a discontinuity in capillary suction. At intermediate suction levels cracks may have a significant influence on moisture transport. Similarly, moisture transport via gas phase transport can be greatly enhanced in unsaturated fracture networks. The behavior of liquid fracture flow is strongly influenced by capillary suction in the adjoining intact porosity, and the focus of subsequent discussion.

Engineered cement-based waste forms and barriers for DOE and NRC applications typically reside (or will reside) in the vadose zone after facility closure, although these barriers will reside above grade during operations. Vadose conditions in humid climates (e.g., Savannah River Site) exhibit relatively low soil suctions, and suggest that cracks in cementitious materials would be important to facility performance. In more arid climates (e.g., Hanford site), cracks may be relatively less important to liquid transport.

A fracture with aperture b can be liquid-filled under the condition:

$$P_\ell > -\frac{2\sigma}{b} \quad (32)$$

where: σ is surface tension and P_ℓ is the liquid pressure imposed by the surrounding matrix and boundary conditions, and suction is indicated by a negative pressure value (Wang & Narasimhan 1985).

The equivalent intrinsic permeability of the fracture is:

$$k' = \frac{b^2}{12} \quad (33)$$

and the saturated liquid hydraulic conductivity is:

$$K_\ell = \frac{\rho_\ell g b^2}{12\eta_\ell} \quad (34)$$

Figure 8 shows hydraulic conductivity as a function of aperture for water at 20°C. Note that even narrow cracks have a high saturated conductivity compared to typical saturated conductivity of cementitious materials ($<10^{-8}$ cm/s).

Although water cannot bridge an aperture when $P_\ell < -2\sigma/b$ and the fracture becomes largely dewatered, non-stationary liquid films may still coat the crack faces. Water flow through a rough walled crack in a porous medium has been documented to occur in at least three distinct regimes (Tokunaga & Wan 1997; Pruess & Tsang 1990; Or & Tuller 2000):

- Saturated flow, that is, liquid completely filling the aperture.
- “Thick” film flow on each crack wall, where water is present as a film completely filling surface pits and grooves and the air-water interface is relatively flat.
- “Thin” film flow, where water recedes into surface pits/grooves by capillary forces and adheres to flat surfaces by adsorption.

The saturated flow regime occurs at positive or very slightly negative pressures. The “thick” and then “thin” film flow regimes occur with increasing suction in the surrounding porous medium.

The full spectrum of flow regimes for idealized fractures has been analyzed theoretically by Or and Tuller (2000) considering uniform crack width and simplified geometry. The authors conceptualize a

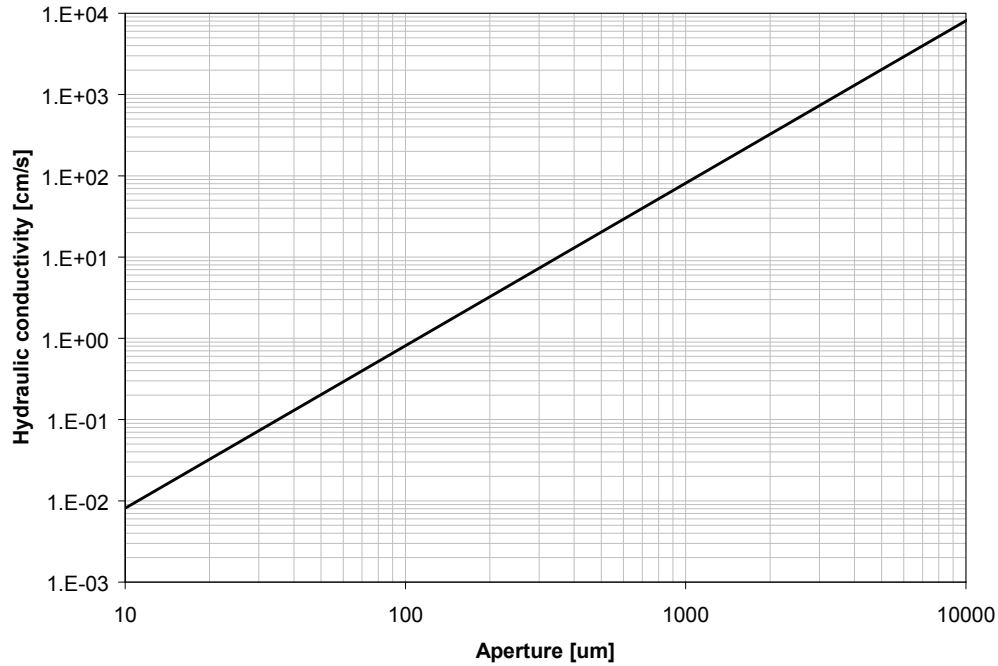


Figure 8: Hydraulic Conductivity of a Saturated Crack as a Function of Aperture

rough fracture face as a repeating series of vertical flat surfaces and V-shaped grooves to facilitate further analysis. At pressures slightly below $-2\sigma/b$, liquid will completely fill a groove and form a flat liquid-vapor interface. At a sufficiently low pressure, liquid will recede into the corner of the groove and be retained by capillary forces. Under this condition, the matric potential determines the radius of the liquid vapor interface in a groove. For a groove of depth L and angle ζ , the maximum radius accommodated by the groove geometry is:

$$r_c = \frac{L \tan(\zeta/2)}{\cos(\zeta/2)} \quad (35)$$

and the critical pressure defining the transition between flat and curved interfaces is:

$$P_{cr} = -\frac{\sigma}{r_c} \quad (36)$$

Thus, the three flow regimes identified earlier occur over the following specific pressure ranges for the assumed geometry of the fracture face:

Saturated flow:

$$P_\ell > -\frac{2\sigma}{b} \quad (37)$$

“Thick” film flow:

$$-\frac{\sigma}{r_c} < P_\ell < -\frac{2\sigma}{b} \quad (38)$$

“Thin” film flow:

$$P_\ell < -\frac{\sigma}{r_c} \quad (39)$$

Liquid not being held by capillary suction in groove corners adheres to the remaining surfaces of the fracture face as a thin film by van der Waal forces. Or and Tuller (2000) show that residual liquid on fracture faces flows downward under the force of gravity. Thus moisture transport is non-zero despite the aperture being mostly de-saturated, an important issue for evaluating the performance of cementitious barriers.

Microcracks with sufficiently small aperture do not enhance transport of water and solutes. Wang et al. (1997) found that crack openings less than 50 μm had “little effect on concrete permeability”, implying a similarly small effect on effective diffusion coefficient. In agreement with the latter, apertures less than about 50 μm did not produce accelerated chloride penetration in cracked concrete (Ismail et al. 2004). In another chloride propagation study, Sahmaran and Yaman (2008) report that “for crack widths less than about 135 μm , the effect of crack width on the effective diffusion coefficient ... was found to be marginal when compared to virgin specimens.”

Larger cracks increase permeability to a widely variable degree (one to several orders of magnitude), depending on the cementitious material, exposure/degradation conditions and resulting crack geometry, and matric suction. Some examples compiled by Černý & Rovnaníková (2002) are reproduced in Table 2.

4.1.1 Modeling Approaches for Fractured Media

The most widely-used approach for simulating moisture transport through a fractured medium at a systems level utilizes a single continuum with effective properties. The effective properties approximate the collective or homogenized behavior of cracks embedded in a porous matrix. Continuum approaches tend to be valid under steady non-localized flow conditions, produce reasonable predictions of average seepage rates (flow integrated across time and/or space), and avoid sophisticated characterization of the fracture network (e.g., (Finsterle 2000; Liu et al. 2003). However, this approach can over-estimate constituent release when coupled with mass transfer of dissolved constituents and local dissolution kinetics or diffusion controls pore water composition (see dual medium approaches below). Effective properties can be derived from

Table 2. Increase in Cracked Concrete Permeability over Uncracked Materials (Černý & Rovnaníková 2002)

Material	MF ^a	Source
30 MPa concrete, comp. stress 70% ult. load	10 ² –10 ⁴	(Kermani 1991)
Ordinary concrete, 100°C	102	(Bazant & Thonguthai 1978)
Ordinary concrete, bending stress, 0.1 mm	2.25	(Bazant, Sener & Kim 1987)
Cement paste, tensile stress, 110 μm	14	(C. Aldea, S. Shah & A. Karr 1999)
Cement mortar, 130 μm , tensile stress	10	(C. Aldea, S. Shah & A. Karr 1999)
Ordinary concrete, 130 μm , tensile stress	2×10 ³	(C. Aldea, S. Shah & A. Karr 1999)
HPC, 110 μm , tensile stress	102	(C. Aldea, S. Shah & A. Karr 1999)
45 MPa concrete, 350 μm , tensile stress	107	(Wang et al. 1997)
45 MPa concrete, 550 μm , tensile stress under load	107	(Wang et al. 1997)
Ordinary concrete, 350 μm , tensile stress under load	2.5×10 ³	(C.M. Aldea, S.P. Shah & A. Karr 1999)
HPC, 300 μm , tensile stress under load	35	(C.M. Aldea, S.P. Shah & A. Karr 1999)
Cement mortar, comp. stress, 90% ult. load	16	(Černý et al. 2000)

^a MF = multiplication factor (i.e., increase in permeability compared to uncracked material).

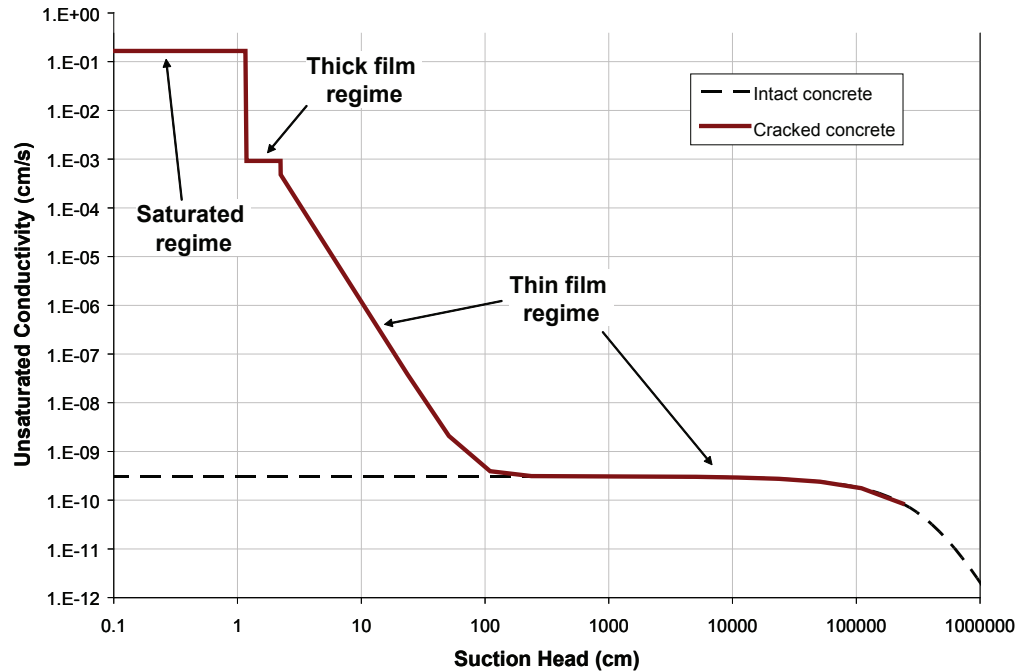


Figure 9: Effective Unsaturated Hydraulic Conductivity Derived for a Hypothetical Cracked Concrete based on Or and Tuller (2000)

Table 3: Selected Parameters for a Hypothetical Cracked Concrete

Parameter	Symbol (Or and Tuller 2000)	Value	Units
ratio of pit spacing to pit depth	b	1	unitless
pit connectivity factor	δ	1	unitless
pit angle	γ	60	deg
pit depth	L	5.0E-04	m
		0.500	mm
		0.020	in
width of unit element	W	1.08E-03	m
aperture	b	1.27E-03	m
		0.05	in
		50	mil
		1.27	mm
		1270	micron
spacing between fractures	B	1	m
		100	cm
saturated matrix conductivity	K	3.1E-12	m/s
		3.1E-10	cm/s
porosity	n	0.18	unitless

experimentation (Persoff & Pruess 1995) or from theoretical or numerical analysis of fracture flow (Pruess & Tsang 1990; Kwicklis & Healy 1993; Liu & Bodvarsson 2001).

As an illustration of the latter, the analysis of Or and Tuller (2000) can be applied to a hypothetical fracture geometry to derive an effective hydraulic conductivity for cracked concrete. An example variation is shown in Figure 9, where for comparison the hydraulic conductivity of uncracked concrete is included. An aperture of 127 μm (5 mil) and crack spacing of 1 cm were chosen, along with the other settings indicated in Table 3. The aperture ($>50 \mu\text{m}$) is large enough to have a significant influence on moisture transport, and the ratio of crack spacing to aperture is 78. G erard & Marchand (2000) define the latter ratio as the *mean crack spacing factor* and note that the parameter “rarely goes below 100, even for concrete samples severely degraded.” Thus the selected crack geometry is representative of severe microcracking. Under saturated flow conditions, the hydraulic conductivity contrast is observed to be nearly 9 orders of magnitude. On the other hand, the cracked and uncracked materials are hydraulically the same for suctions exceeding about 100 cm. At intermediate suction levels, between 1 and 100 cm, the influence of cracks is strongly dependent on suction.

Motivated primarily by solute rather than water transport considerations, a fractured porous medium is often separated conceptually into separate, but spatially overlapping, matrix and fracture continuum domains (or porosities). The *dual-porosity* concept has been applied to several physical settings, including laboratory soil columns, heterogeneous granular aquifers, aggregated media, and in the situation most relevant to the present, fractured geologic media (Passioura 1971; Skopp & Warrick 1974; van Genuchten & Wierenga 1976; van Genuchten & Wierenga 1977; van Genuchten,

Wierenga & O’Connor 1977; Rao et al. 1980; Hayot & Lafolie 1993; Lafolie & Hayot 1993; Brusseau et al. 1994; Griffioen, Barry & Parlange 1998). Specific formulations range from *mobile-immobile* regions with first-order mass transfer (Coats and Smith, 1964) to *dual-permeability*, in which advection occurs in both regions (Gerke & van Genuchten 1993). Generalizations of the concept have also been developed (Haggerty and Gorelick 1995, Wang et al. 2005). Dual-porosity formulations generally assume that all water transport occurs in fractures and none in the matrix, while dual-permeability implies moisture movement in both domains. Effective porous medium properties are required for the active domain(s), analogous to single-domain modeling.

In *Discrete Fracture Modeling (DFM)* flow is explicitly simulated through individual fractures, as well as the surrounding matrix (Yu, Ruiz & Chaves 2008; Kim & Deo 2000). DFM preserves the physical geometry of fractures, or at least approximately in terms of key attributes such as aperture, spacing and connectivity. The approach offers a more accurate representation of the physical system, at the expense of additional effort to characterize the fracture network and significantly higher computational demands. In practice, single- or dual-continuum models are typically chosen for system level or field scale modeling, while discrete fracture modeling is better suited to laboratory or small scale simulations.

5.0 OTHER TRANSPORT MODELS

5.1 Pore-Scale Models

Pore-scale models explicitly model flow processes occurring on the scale of pores. While this level of detail is computationally impractical for simulating integrated effects over much larger scales, pore-scale models are of interest for studying key phenomena at the microscale.

Since water migration through cementitious materials primarily depends upon capillary potential, many researchers have utilized the Hagen-Poiseuille relation to model liquid transport on a fundamental mechanistic level (Capek et al. 2007; Martys & Ferraris 1997; Song & Kwon 2007; Leventis et al. 2000). The Hagen-Poiseuille relation expresses the fluid flux j [m^3/s] in a capillary tube as a function of pressure drop $\Delta P \Delta P_\ell$ [Pa], given as (Leventis et al. 2000).

$$j = \frac{\pi \left(\frac{d^4}{2} \right) \Delta P_\ell}{8\eta l} \quad (40)$$

where: d is the diameter of the pore [m], l is the length of the pore [m], η is the dynamic viscosity of the fluid [Pa·s]. These models greatly simplify pore geometry by conceptualizing pores as orthogonally interconnected cylinders or cubes, for which the Poiseuille equation has an exact analytical solution.

The orthogonal nature of such models lends their use to three-dimensional determination of fluid flow but inherently necessitates empirical correction factors for tortuosity or connectivity of pores. Generation of these network models is accomplished either by randomly selecting pore size and connectivity based upon real pore-size distribution data (Garboczi 1991; Kainourgiakis et al. 2005; Oren & Bakke 2003; Pradhan, Nagesh & Bhattacharjee 2005) or by tracing the void spaces in tomographed images of real materials (Carmeliet et al. 2004). The main advantage of using such a network lies in computing transport through macro-pores ($\geq 20 \mu\text{m}$) which exhibit open-channel flow behavior (Roels, Vandersteen & Carmeliet 2003). A major limitation of these models is the difficulty in quantifying water migration through gel pores ($\approx 2 \text{ nm}$ diameter) in a mechanistic manner.

Researchers have combated this problem by superimposing a 3-D cubic macropore network, a capillary pore continuum, and a nano-scale pore network (Philippi & Souza 1995). It is important to note that cylindrical pore networks are useful only for the calculation of the phenomenon upon which they are calibrated and are not representative of true pore geometry (Garboczi 1991). Therefore, determination of transport rates that depend on other physical and chemical characteristics, such as phase surface area, must be accounted for explicitly in the model.

5.2 Lattice-Boltzmann Methods

The lattice-Boltzmann modeling approach presents an elegant yet computationally intensive method for determining multi-phase fluid transport parameters in porous media. The lattice-Boltzmann method is a numerical simulation technique that allows for the movement, and subsequent collisions, of particles along a regular lattice. Collisions are deterministic and governed by rules so as to conserve number of particles and momentum (McNamara & Zanetti 1988). The method entails discretizing an entire pore space into static nodes of solid phase and dynamic nodes of fluid phases (typically one wetting phase and one non-wetting phase). Martys and Hagedorn implemented the lattice-Boltzmann approach on tomographic reconstructions of sandstone and cracked mortars (Martys & Hagedorn 2002). Lattice-Boltzmann routines have the advantage of being adaptable to any spatial scale, but rely on accurate model representations of physical pore structure. The heterogeneity of porous microstructures across length scales presents a challenge for delineating single lattice spacing. One method of dealing with this problem is discretizing the larger pores and treating the smaller pores as a permeable continuum which obeys Darcy's law. The boundary conditions at

interfaces between the larger pores and the permeable medium are determined by the Brinkman equation which satisfies both the continuity equation and the shear stress condition (Martys & Hagedorn 2002).

6.0 CHALLENGES AND OPPORTUNITIES

The fundamentals of moisture transport in cementitious materials are well understood, and a variety of effective modeling approaches have been advanced for predicting moisture movement. The Cementitious Barriers Partnership will likely choose a single- or dual-domain continuum formulation for macroscale moisture transport simulation. At smaller scales, discrete fracture and/or pore-scale models are likely to be useful for estimating effective parameters and understanding specific coupled phenomena.

Accurate simulations do depend on adequate characterization of key physical properties, typically defined by empirical relationships requiring experimental testing. The key properties for moisture transport simulation include:

- hydraulic conductivity (permeability) in saturated and unsaturated materials,
- hydraulic diffusivity as a function of water content, and
- water retention curves (water content or saturation as a function of relative humidity)

While established techniques are available for measuring the porous medium properties of intact undamaged laboratory specimens, characterization of damaged (e.g., fractured) cementitious materials will be a challenge. When damage is in the form of cracking, complete characterization may encompass definition of aperture distribution, spacing, orientation, connectivity, asperity, etc., which may be useful for system conceptualization and model validation but are impractical for long-

term prediction. Large samples may be required to define representative properties. Furthermore, in many Cementitious Barriers Partnership applications of interest, damage will evolve over many thousands of years, such that representative contemporary specimens are not available for direct testing.

Thus, the primary challenge to accurate moisture simulation will be adequate definition of hydraulic properties and how these properties evolve in response to physical and chemical changes and stresses imposed on the system.

These challenges create opportunities for devising accelerated degradation tests and innovative experiments at the laboratory and field scales to define the hydraulic properties of damaged cementitious materials.

7.0 REFERENCES

- Aldea, C, Shah, S & Karr, A 1999, 'Permeability of cracked concrete', *Materials and Structures*, vol. 32, no. 5, pp. 370-376.
- Aldea, CM, Shah, SP & Karr, A 1999, 'Effect of cracking on water and chloride permeability of concrete', *Journal of Materials in Civil Engineering*, vol. 11, pp. 181-187.
- Anderberg, A & Wadsö, L 2008, 'Method for simultaneous determination of sorption isotherms and diffusivity of cement-based materials', *Cement and Concrete Research*, vol. 38, no. 1, pp. 89-94.
- ASTM E96 2005, Standard Test Method for Water Vapor Transmission of Materials, ASTM International, West Conshohocken, PA.
- Baroghel-Bouny, V 2007a, 'Water vapour sorption experiments on hardened cementitious materials. Part II: Essential tool for assessment of transport properties and for durability prediction', *Cement and Concrete Research*, vol. 37, no. 3, pp. 438-454.
- Baroghel-Bouny, V 2007b, 'Water vapour sorption experiments on hardened cementitious materials: Part I: Essential tool for analysis of hygral behaviour and its relation to pore structure', *Cement and Concrete Research*, vol. 37, no. 3, pp. 414-437.
- Bazant, ZP & Najjar, LJ 1971, 'Drying of concrete as a nonlinear diffusion problem', *Cement and Concrete Research*, vol. 1, no. 5, pp. 461-473.
- Bazant, ZP, Sener, S & Kim, JK 1987, 'Effect of cracking on drying permeability and diffusivity of concrete', *ACI Materials Journal*, vol. 84, pp. 351-357.
- Bazant, ZP & Thonguthai, W 1978, 'Pore pressure and drying of concrete at high temperatures', *Journal of Engineering Mechanics Division ASCE*, vol. 104, pp. 1059-1079.
- Bear, J 1972, *Dynamics of Fluids in Porous Media*, American Elsevier, New York.
- Bear, J & Buchlin, J-M (eds) 1991, *Modelling and Applications of Transport Phenomena in Porous Media.*, Springer.
- Blümich, B 2000, *NMR Imaging of Materials*, Oxford University Press, New York.
- Brusseau, ML, Gerstl, Z, Augustijn, D & Rao, PSC 1994, 'Simulating solute transport in an aggregated soil with the dual-porosity model: measured and optimized parameter values', *Journal of Hydrology*, vol. 163, no. 1-2, pp. 187-193.
- Capek, P, Hejtmanek, V, Brabec, L, Zikanova, A & Kocirik, M 2007, 'Network modelling of capillary pressure curves, permeability, and diffusivity', *Chemical Engineering Science*, vol. 62, no. 18-20, pp. 5117-5122.
- Carmeliet, J, Delerue, JF, Vandersteen, K & Roels, S 2004, 'Three-dimensional liquid transport in concrete cracks', *International Journal for Numerical and Analytical Methods in Geomechanics*, vol. 28, no. 7-8, pp. 671-687.
- Černý, R, Madera, J, Podebradská, J, Toman, J, Drchalová, J, Klecka, T, Jurek, K & Rovnaníková, P 2000, 'The effect of compressive stress on thermal and hygric properties of Portland cement mortar in wide temperature and moisture ranges', *Cement and Concrete Research*, vol. 30, no. 8, pp. 1267-1276.

- Černý, R & Rovnaníková, P 2002, *Transport Processes in Concrete*, Spon Press, New York.
- Christensen, BJ, Mason, TO & Jennings, HM 1996, 'Comparison of measured and calculated permeabilities for hardened cement pastes', *Cement and Concrete Research*, vol. 26, no. 9, pp. 1325-1334.
- Cnudde, V, Dierick, M, Vlassenbroeck, J, Masschaele, B, Lehmann, E, Jacobs, P & Van Hoorebeke, L 2008, 'High-speed neutron radiography for monitoring the water absorption by capillarity in porous materials', *Nuclear Instruments and Methods in Physics Research Section B: Beam Interactions with Materials and Atoms*, vol. 266, no. 1, pp. 155-163.
- Crank, J 1975, *The Mathematics of Diffusion*, Oxford University Press, London, UK.
- CRD 1992a, *Standard Test Method for Water Permeability of Concrete* in Handbook of Cement and Concrete, US Army Corp of Engineers.
- CRD 1992b, Standard Test Method for Water Permeability of Concrete using Triaxial Cell, US Federal Standards.
- Cui, L & Cahyadi, JH 2001, 'Permeability and pore structure of OPC paste', *Cement and Concrete Research*, vol. 31, no. 2, pp. 277-282.
- Dao, VNT, Morris, PH & Dux, PF 2008, 'On equations for the total suction and its matric and osmotic components', *Cement and Concrete Research*, vol. 38, no. 11, pp. 1302-1305.
- de Marsily, G 1986, *Quantitative Hydrogeology: Groundwater Hydrology for Engineers*, Academic Press, New York.
- Diamond, S 2000, 'Mercury porosimetry: An inappropriate method for the measurement of pore size distributions in cement-based materials', *Cement and Concrete Research*, vol. 30, no. 10, pp. 1517-1525.
- El-Dieb, AS & Hooton, RD 1994a, 'Evaluation of the Katz-Thompson model for estimating the water permeability of cement-based materials from mercury intrusion porosimetry data', *Cement and Concrete Research*, vol. 24, no. 3, pp. 443-455.
- El-Dieb, AS & Hooton, RD 1994b, 'A high pressure triaxial cell with improved measurement sensitivity for saturated water permeability of high performance concrete', *Cement and Concrete Research*, vol. 24, no. 5, pp. 854-862.
- El-Dieb, AS & Hooton, RD 1995, 'Water-permeability measurement of high performance concrete using a high-pressure triaxial cell', *Cement and Concrete Research*, vol. 25, no. 6, pp. 1199-1208.
- Erlin, B & Mather, B 2005, 'A new process by which cyclic freezing can damage concrete--the Erlin/Mather effect a concept', *Cement and Concrete Research*, vol. 35, no. 7, pp. 1407-1411.
- Feldman, RF 1984, 'Pore structure damage in blended cements caused by mercury intrusion', *Journal of the American Ceramic Society*, vol. 67, no. 1, pp. 30-33.
- Finsterle, S 2000, 'Using the continuum approach to model unsaturated flow in fractured rock', *Water Resources Research*, vol. 36, no. 8, pp. 2055-2066.
- Fredlund, DG & Rahardjo, H 1993, *Soils Mechanics for Unsaturated Soils*, John Wiley, New York.
- Gambhir, ML 2004, *Concrete Technology*, Tata McGraw-Hill, New Delhi.

- Garbalinska, H 2006, 'Application of \sqrt{t} -type, logarithmic and half-time methods in desorptive measurements of diffusivity in narrow humidity ranges', *Cement and Concrete Research*, vol. 36, no. 7, pp. 1294-1303.
- Garboczi, EJ 1990, 'Permeability, diffusivity, and microstructural parameters: A critical review', *Cement and Concrete Research*, vol. 20, no. 4, pp. 591-601.
- Garboczi, EJ 1991, 'Mercury porosimetry and effective networks for permeability calculations in porous materials', *Powder Technology*, vol. 67, no. 2, pp. 121-125.
- Garrabrants, AC & Kosson, DS 2003, 'Modeling moisture transport from a portland cement-based material during storage in reactive and inert atmospheres', *Drying Technology*, vol. 21, no. 5, pp. 775 - 805[October 01, 2008].
- Gawin, D, Pesavento, F & Schrefler, BA 2006, 'Towards prediction of the thermal spalling risk through a multi-phase porous media model of concrete', *Computer Methods in Applied Mechanics and Engineering*, vol. 195, no. 41-43, pp. 5707-5729.
- Gerard, B & Marchand, J 2000, 'Influence of cracking on the diffusion properties of cement-based materials: Part I: Influence of continuous cracks on the steady-state regime', *Cement and Concrete Research*, vol. 30, no. 1, pp. 37-43.
- Gerke, H & van Genuchten, MT 1993, 'A dual-porosity model for simulating the preferential movement of water and solutes in structured porous media', *Water Resources Research*, vol. 29, no. 2, pp. 305-319.
- Grasley, ZC, Scherer, GW, Lange, DA & Valenza, JJ 2007, 'Dynamic pressurization method for measuring permeability and modulus: II. Cementitious materials', *Materials and Structures*, vol. 40, no. 7, pp. 711-721.
- Griffioen, J, Barry, D & Parlange, J-Y 1998, 'Interpretation of two region model parameters', *Water Resources Research*, vol. 34, no. 3, pp. 373-384.
- Gummerson, RJ, Hall, C, Hoff, WD, Hawkes, R, Holland, GN & Moore, WS 1979, 'Unsaturated water flow within porous materials observed by NMR imaging', *Nature*, vol. 281, no. 5726, pp. 56-57.
- Hagymassy, J, Odler, I, Yudenfreund, M, Skalny, J & Brunauer, S 1972, 'Pore structure analysis by water vapor adsorption. III. Analysis of hydrated calcium silicates and portland cements', *Journal of Colloid and Interface Science*, vol. 38, no. 1, pp. 20-34.
- Halamickova, P, Detwiler, RJ, Bentz, DP & Garboczi, EJ 1995, 'Water permeability and chloride ion diffusion in portland cement mortars: Relationship to sand content and critical pore diameter', *Cement and Concrete Research*, vol. 25, no. 4, pp. 790-802.
- Hall, C & Hoff, W 2002, *Water Transport in Brick, Stone and Concrete*, Spon Press, New York.
- Hayot, C & Lafolie, F 1993, 'One-dimensional solute transport modelling in aggregated porous media Part 2. Effects of aggregate size distribution', *Journal of Hydrology*, vol. 143, no. 1-2, pp. 85-107.
- Hazrati, K, Pel, L, Marchand, J, Kopinga, K & Pigeon, M 2002, 'Determination of isothermal unsaturated capillary flow in high performance cement mortars by NMR imaging', *Materials and Structures*, vol. 35, no. 10, pp. 614-622.
- Hearn, N & Mills, RH 1991, 'A simple permeameter for water or gas flow', *Cement and Concrete Research*, vol. 21, no. 2-3, pp. 257-261.
- Hope, BB & Malhotra, VM 1984, 'The measurement of concrete permeability', *Canadian Journal of Civil Engineering*, vol. 11, no. 2, pp. 287-292.

- Ismail, M, Toumi, A, François, R & Gagné, R 2004, 'Effect of crack opening on the local diffusion of chloride in inert materials', *Cement and Concrete Research*, vol. 34, no. 4, pp. 711-716.
- Jones, CA & Grasley, ZC 2009, 'Correlation of hollow and solid cylinder dynamic pressurization tests for measuring permeability', *Cement and Concrete Research*, vol. 39, no. 4, pp. 345-352.
- Kainourgiakis, ME, Kikkinides, ES, Galani, A, Charalambopoulou, GC & Stubos, AK 2005, 'Digitally reconstructed porous media: Transport and sorption properties', *Transport in Porous Media*, vol. 58, no. 1, pp. 43-62.
- Katz, AJ & Thompson, AH 1986, 'Quantitative prediction of permeability in porous rock', *Physical Review B*, vol. 34, no. 11, p. 8179.
- Kermani, A 1991, 'Permeability of stressed concrete', *Building Research and Information*, vol. 19, pp. 360-366.
- Ketelaars, AAJ, Pel, L, Coumans, WJ & Kerkhof, PJAM 1995, 'Drying kinetics: A comparison of diffusion coefficients from moisture concentration profiles and drying curves', *Chemical Engineering Science*, vol. 50, no. 7, pp. 1187-1191.
- Kim, J-G & Deo, MD 2000, 'Finite element, discrete-fracture model for multiphase flow in porous media', *AIChE Journal*, vol. 46, no. 6, pp. 1120-1130.
- Kwicklis, E & Healy, R 1993, 'Numerical investigation of steady liquid water flow in a variably saturated fracture', *Water Resources Research*, vol. 29, no. 12, pp. 4091-4102.
- Lafolie, F & Hayot, C 1993, 'One-dimensional solute transport modelling in aggregated porous media Part 1. Model description and numerical solution', *Journal of Hydrology*, vol. 143, no. 1-2, pp. 63-83.
- Leech, C, Lockington, D & Dux, P 2003, 'Unsaturated diffusivity functions for concrete derived from NMR images', *Materials and Structures*, vol. 36, no. 6, pp. 413-418.
- Leventis, A, Verganelakis, DA, Halse, MR, Webber, JB & Strange, JH 2000, 'Capillary imbibition and pore characterisation in cement pastes', *Transport in Porous Media*, vol. 39, no. 2, pp. 143-157.
- Liu, H-H & Bodvarsson, GS 2001, 'Constitutive relations for unsaturated flow in a fracture network', *Journal of Hydrology*, vol. 252, no. 1-4, pp. 116-125.
- Liu, H-H, Haukwa, CB, Ahlers, CF, Bodvarsson, GS, Flint, AL & Guertal, WB 2003, 'Modeling flow and transport in unsaturated fractured rock: an evaluation of the continuum approach', *Journal of Contaminant Hydrology*, vol. 62-63, pp. 173-188.
- Lockington, D, Parlange, J & Dux, P 1999, 'Sorptivity and the estimation of water penetration into unsaturated concrete', *Materials and Structures*, vol. 32, no. 5, pp. 342-347.
- Mainguy, M, Coussy, O & Baroghel-Bouny, V 2001, 'Role of air pressure in drying of weakly permeable materials', *Journal of Engineering Mechanics*, vol. 127, no. 6, pp. 582-592.
- Martys, NS & Ferraris, CF 1997, 'Capillary transport in mortars and concrete', *Cement and Concrete Research*, vol. 27, no. 5, pp. 747-760.
- Martys, NS & Hagedorn, JG 2002, 'Multiscale modeling of fluid transport in heterogeneous materials using discrete Boltzmann methods', *Materials and Structures*, vol. 35, pp. 650-649.
- Matano, C 1932-33, 'On the relation between the diffusion-coefficients and concentrations of solid metals (the nickel-copper system)', *Japanese Journal of Physics*, vol. 8, pp. 109-113.

- McArthur, H & Spalding, D 2004, *Engineering Materials Science: Properties, Uses, Degradation and Remediation*, 577 vols, Horwood.
- McNamara, GR & Zanetti, G 1988, 'Use of the Boltzmann equation to simulate lattice-gas automata', *Physical Review Letters*, vol. 61, no. 20, p. 2332.
- Mensi, R, Acker, P & Attolou, A 1988, 'Séchage du béton: analyse et modélisation', *Materials and Structures*, vol. 21, no. 1, pp. 3-12.
- Moro, F & Bohni, H 2002, 'Ink-bottle effect in mercury intrusion porosimetry of cement-based materials', *Journal of Colloid and Interface Science*, vol. 246, no. 1, pp. 135-149.
- Mosquera, MJ, Silva, B, Prieto, B & Ruiz-Herrera, E 2006, 'Addition of cement to lime-based mortars: Effect on pore structure and vapor transport', *Cement and Concrete Research*, vol. 36, no. 9, pp. 1635-1642.
- Mualem, Y 1976, 'A new model for predicting the hydraulic conductivity of unsaturated porous media', *Water Resources Research*, vol. 12, no. 3, pp. 513-522.
- Nilsson, L-O 2003, 'Durability concept: Pore structure and transport processes', in *Advanced Concrete Technology: Concrete Properties*, eds JB Newman & BS Choo, Butterworth-Heinemann.
- Nokken, M & Hooton, R 2006, 'Using pore parameters to estimate permeability or conductivity of concrete', *Materials and Structures*.
- Nokken, M & Hooton, R 2008, 'Using pore parameters to estimate permeability or conductivity of concrete', *Materials and Structures*, vol. 41, no. 1, pp. 1-16.
- Olson, RA, Neubauer, CM & Jennings, HM 1997, 'Damage to the pore structure of hardened portland cement paste by mercury intrusion', *Journal of the American Ceramic Society*, vol. 80, no. 9, pp. 2454-2458.
- Or, D & Tuller, M 2000, 'Flow in unsaturated fractured porous media: Hydraulic conductivity of rough surfaces', *Water Resources Research*, vol. 36, no. 5, pp. 1165-1177.
- Oren, P-E & Bakke, S 2003, 'Reconstruction of Berea sandstone and pore-scale modelling of wettability effects', *Journal of Petroleum Science and Engineering*, vol. 39, no. 3-4, pp. 177-199.
- Passioura, J 1971, 'Hydrodynamic dispersion in aggregated media: 1. Theory', *Soil Science*, vol. 3, no. 6, pp. 339-344.
- Pel, L, Hazrati, K, Kopinga, K & Marchand, J 1998, 'Water absorption in mortar determined by NMR', *Magnetic Resonance Imaging*, vol. 16, no. 5-6, pp. 525-528.
- Pel, L, Ketelaars, AAJ, Adan, OCG & Van Well, AA 1993, 'Determination of moisture diffusivity in porous media using scanning neutron radiography', *International Journal of Heat and Mass Transfer*, vol. 36, no. 5, pp. 1261-1267.
- Persoff, P & Pruess, K 1995, 'Two-phase flow visualization and relative permeability measurement in natural rough-walled rock fractures', *Water Resources Research*, vol. 31, no. 5, pp. 1175-1186.
- Philippi, PC & Souza, HA 1995, 'Modelling moisture distribution and isothermal transfer in a heterogeneous porous material', *International Journal of Multiphase Flow*, vol. 21, no. 4, pp. 667-691.

- Pradhan, B, Nagesh, M & Bhattacharjee, B 2005, 'Prediction of the hydraulic diffusivity from pore size distribution of concrete', *Cement and Concrete Research*, vol. 35, no. 9, pp. 1724-1733.
- Pruess, K & Tsang, YW 1990, 'On two-phase relative permeability and capillary pressure of rough-walled rock fractures', *Water Resources Research*, vol. 26, no. 9, pp. 1915-1926.
- Rao, PSC, Rolston, DE, Jessup, RE & Davidson, JM 1980, 'Solute transport in aggregated porous media: Theoretical and experimental evaluation', *Soil Science Society of America Journal*, vol. 44, pp. 1139-1146.
- Richards, BG 1965, 'Measurement of free energy of soil moisture by the psychrometric technique using thermistors', *Moisture Equilibria and Moisture Changes in Soils Beneath Covered Areas: A Symposium*.
- Roels, S, Vandersteen, K & Carmeliet, J 2003, 'Measuring and simulating moisture uptake in a fractured porous medium', *Advances in Water Resources*, vol. 26, no. 3, pp. 237-246.
- Samson, E, Maleki, K, Marchand, J & Zhang, T 2008, 'Determination of the water diffusivity of concrete using drying/adsorption test results', *Journal of the ASTM International*, vol. 5.
- Savage, BM & Janssen, DJ 1997, 'Soil physics principles validated for use in predicting unsaturated moisture movement in portland cement concrete', *ACI Materials Journal*, vol. 94, no. 1, pp. 63-70.
- Scherer, GW 1999, 'Crystallization in pores', *Cement and Concrete Research*, vol. 29, no. 8, pp. 1347-1358.
- Scherer, GW 2006, 'Dynamic pressurization method for measuring permeability and modulus: I. Theory', *Materials and Structures*, vol. 39, no. 10, pp. 1041-1057.
- Scherer, GW, Valenza, JJ, II & Simmons, G 2007, 'New methods to measure liquid permeability in porous materials', *Cement and Concrete Research*, vol. 37, no. 3, pp. 386-397.
- Šelih, J, Sousa, ACM & Bremner, TW 1996, 'Moisture transport in initially fully saturated concrete during drying', *Transport in Porous Media*, vol. 24, no. 1, pp. 81-106.
- Skopp, J & Warrick, AW 1974, 'A two-phase model for the miscible displacement of reactive solutes in soils', *Soil Science Society of America Journal*, vol. 38, pp. 545-550.
- Snyder, KA & Marchand, J 2001, 'Effect of speciation on the apparent diffusion coefficient in nonreactive porous systems', *Cement and Concrete Research*, vol. 31, no. 12, pp. 1837-1845.
- Song, H-W & Kwon, S-J 2007, 'Permeability characteristics of carbonated concrete considering capillary pore structure', *Cement and Concrete Research*, vol. 37, no. 6, pp. 909-915.
- Tokunaga, TK & Wan, J 1997, 'Water film flow along fracture surfaces in porous rock', *Water Resources Research*, vol. 33, no. 6, pp. 1287-1295.
- Tumidajski, PJ & Lin, B 1998, 'On the validity of the Katz-Thompson equation for permeabilities in concrete', *Cement and Concrete Research*, vol. 28, no. 5, pp. 643-647.
- van Genuchten, MT 1980, 'A closed-form equation for predicting the hydraulic conductivity of unsaturated soils', *Soil Science Society of America Journal*, vol. 44, no. 5, pp. 892-898.
- van Genuchten, MT & Wierenga, PJ 1976, 'Mass transfer studies in sorbing porous media I. Analytical solutions', *Soil Science Society of America Journal*, vol. 40, pp. 473-480.

- van Genuchten, MT & Wierenga, PJ 1977, 'Mass transfer studies in sorbing porous media II. Experimental evaluation with tritium ($3\text{H}_2\text{O}$)', *Soil Science Society of America Journal*, vol. 41, pp. 272-278.
- van Genuchten, MT, Wierenga, PJ & O'Connor, GA 1977, 'Mass transfer studies in sorbing porous media III. Experimental evaluation with $2,3,4\text{-T}$ ', *Soil Science Society of America Journal*, vol. 41, pp. 278-285.
- Vichit-Vadakan, W & Scherer, GW 2002, 'Measuring permeability of rigid materials by beam-bending method: III. Cement paste', *Journal of the American Ceramic Society*, vol. 85, pp. 1537-1544.
- Wang, J & Narasimhan, T 1985, 'Hydrologic mechanisms governing fluid flow in a partially saturated fractured, porous medium', *Water Resources Research*, vol. 21, no. 12, pp. 1861-1874.
- Wang, K, Jansen, DC, Shah, SP & Karr, AF 1997, 'Permeability study of cracked concrete', *Cement and Concrete Research*, vol. 27, no. 3, pp. 381-393.
- Wardeh, G & Perrin, B 2006, 'Relative permeabilities of cement-based materials: Influence of the tortuosity function', *Journal of Building Physics*, vol. 30, no. 1, pp. 39-57.
- Webb, SW 2006, 'Two-phase gas transport', in *Gas Transport in Porous Media*, eds CK Ho & SW Webb, Springer, New York, pp. 55-70.
- Xi, Y, Bazant, ZP, Molina, L & Jennings, HM 1994, 'Moisture diffusion in cementitious materials Moisture capacity and diffusivity', *Advanced Cement Based Materials*, vol. 1, no. 6, pp. 258-266.
- Yu, RC, Ruiz, G & Chaves, EWV 2008, 'A comparative study between discrete and continuum models to simulate concrete fracture', *Engineering Fracture Mechanics*, vol. 75, no. 1, pp. 117-127.

8.0 APPENDIX: MATERIAL PROPERTIES DEFINING THE PHYSICAL STATE OF A POROUS-MEDIUM

Property	Symbol	Definition
Porosity		
total	ϕ	void volume divided by total volume
open/connected	ϕ_o	porosity with connection to external boundaries that is occupied by air and/or water that is not chemically or physically bound to cement
closed/unconnected	ϕ_c	porosity without connection to external boundaries or occupied by water that is chemically or physically bound to cement
effective	ϕ_e	porosity through which primary (e.g., advective) solute transport occurs for particular time and spatial scales
Permeability		
intrinsic	κ	flow proportionality coefficient that is independent of fluid properties and defined through a form of Darcy's law: $U = -(\kappa \rho g k_r / \eta_\ell) \nabla h$
relative	$k_r \langle S \theta \rangle$	water or air permeability under unsaturated conditions relative to the saturated condition; may be defined as a function of saturation or water content
Hydraulic Conductivity		
(water or air) saturated	K	flow proportionality coefficient dependent on fluid properties and defined for through a form of Darcy's law: $U = -K k_r \nabla h$
unsaturated	$K k_r$	hydraulic conductivity under unsaturated conditions
hydraulic diffusivity	$D_\theta \langle \theta \rangle$	flow proportionality coefficient defined by: $D_\theta = -K_\ell k_{r\ell} \frac{dh_c}{d\theta}$
water retention	$S \theta \langle h_c \rangle$	saturation or water content as a function of capillary suction head
Diffusion Coefficient		
molecular	D_m	proportionality coefficient for diffusive transport in open/free fluid
effective	D_e	diffusion coefficient accounting for slower transport due to flow path tortuosity in a porous medium: $D_e = D/\tau$
intrinsic	D_i	diffusion coefficient accounting for tortuosity and flow area reduction due the presence of solids (porosity): $D_i = \phi D_e = \phi D/\tau$
apparent	D_a	diffusion coefficient accounting for tortuosity, porosity, and solute sorption/binding
Tortuosity		
tortuosity	τ	diffusion rate through open water relative to saturated pore space (comprising tortuous flow paths)
Solid Density		
particle	ρ_s	mass of solid per unit volume of solid
bulk	ρ_b	mass of solid per unit volume of sample
Fluid Properties		
fluid density	ρ_f	fluid (water or air) mass per unit volume of fluid
fluid viscosity	η_f	measure of fluid (water or air) resistance in response to shear stress



U.S. DEPARTMENT OF
ENERGY

